EPRI
Palo Alto, California

COMBUSTION TURBINE (CT) HOT SECTION COATING LIFE MANAGEMENT

Semi Annual Technical Progress Report

Reporting Period Start Date: April 1, 2003
Reporting Period End Date: September 30, 2003

Agreement Number: **DE-FC26-01NT41231**

Principal Authors:
R. Viswanathan
D. Gandy
K. Krzywosz
S. Cheruvu
E. Wan

Subcontractors

Southwest Research Institute
Turbine Technology International

Submitted by
R. Viswanathan/D. Gandy
EPRI
3412 Hillview Avenue
Palo Alto, CA 94304
September 15, 2003
Email: rviswana@epri.com

Disclaimer

"This (describe material) was prepared with the support of the U.S. Department of Energy, under Award No. DE-FC26-01NT41231. However, any opinions, findings, conclusions, or recommendations expressed herein are those of the author(s) and do not necessarily reflect the views of the DOE".

TABLE OF CONTENTS

LIST OF TABLES

LIST OF FIGURES

COMBUSTION TURBINE (CT) HOT SECTION COATING LIFE MANAGEMENT

1.0 ABSTRACT

The integrity of coatings used in hot section components of combustion turbines is crucial to the reliability of the buckets. This project was initiated in recognition of the need for predicting the life of coatings analytically, and non-destructively; correspondingly, three principal tasks were established. Task 1, with the objective of analytically developing stress, strain and temperature distributions in the bucket and thereby predicting thermal fatigue (TMF) damage for various operating conditions; Task 2 with the objective of developing eddy current techniques to measure both TMF damage and general degradation of coatings and, Task 3 with the objective of developing mechanism based algorithms. Task 4 would be aimed at verifying analytical predictions from Task 1 and the NDE predictions from Task 3 against field observations. Task 5 would develop a rislk-based decision analysis model to make run/repair decisions. This report is a record of the progress to date on these four tasks.

2.0 INTRODUCTION

The objective of this project is to improve the reliability, availability and maintainability (RAM) of combustion turbines (GTs) by developing advanced technology for assessing and managing the life of protective coatings on CT blades and vanes.

In recent years, gas turbines (GTs) have become the equipment of choice for power generation by both electric utilities and independent power producers. Continuing advances in design concepts and in structural materials and coatings for GT hot-section components have enabled increases in rotor inlet temperature resulting in major efficiency gains. These high temperatures mandate the use of coatings on hot section components (blades and vanes) to protect them from oxidation. Degradation of these protective coatings represents a major profitability challenge for turbine owners. Coating life usually dictates blade refurbishment intervals – which typically are shorter than desired for baseload units. Downtime for coating inspection and replenishment requires dispatch of less efficient generating equipment or purchase of replacement power. Coating failure can lead to rapid, severe damage to the superalloy substrate, warranting blade replacement. Replacement of a conventionally cast alloy blade row can cost up to $3 million in the case of directionally solidified or single-crystal blades with internal cooling. Unavailability costs can run up to $500,000 in lost revenues per day for a 500MW combined cycle plant. Blade failures can also cause downstream damage in the turbine, causing prolonged outages and revenue loss. Moreover, losses to electricity customers due to disruption in supply can also be very substantial. A proper life management system for coatings represents a major step in preventing such major losses to the GT owner and to society at large.

The life management activities covered in this project for coatings directly impacts the objectives of increasing RAM of GTs. Accurate life management techniques optimize refurbishment intervals and operating practices, thereby avoiding unplanned outages. Currently, coating refurbishment intervals are dictated by empirical, fleet-specific (rather than unit-specific) manufacturer recommendations based on the concept of "equivalent operating hours (EOH)." The new technology described in this proposal will enable machine-specific calculations of coating remaining life and direct measurements of the same using non-destructive evaluation (NDE) techniques.

The project is intended to develop improved analytical and nondestructive evaluation techniques to assess the consumed life and/or estimated life of protective coatings on CT blades and vanes, and then integrate these techniques with economic risk-based decision-analysis tools to optimize run/repair/replace decisions. The project is defined along five major technical tasks including:

Task 1. Refinement and Validation of Hot Section Life Management Platform (HSLMP)
Task 2. COATLIFE for Advanced Metallic Coatings and TBCs
Task 3. NDE of Coatings
Task 4. Field Validation of COATLIFE and NDE
Task 5. Economic risk-based Decision Analysis

This report summarizes results from these tasks.

3.0 EXECUTIVE SUMMARY

In Task 1 the primary objective for the period 04/01/03-09/30/03 was to perform damage assessment for S-W W501FC 1st stage bucket. Thermal-mechanical fatigue (TMF), creep and TBC life analyses were performed based on aero-thermal results and life model developed by EPRI/SwRI. Thermal transients investigated for various operating cycles included startup, normal shutdown and full load trip. At the platform where cracking has occurred, the strain range was calculated to be 0.6% and the corresponding TMF life was predicted to be about 150 cycles. These assumed a normal startup and shutdown mode. The excessive compressive stress at base load is a result of highly non-uniform temperature distributions, and is most damaging in terms of TMF life. The platform through-thickness crack is concluded to be the life-limiting factor that dictates replacement and repair interval of the 1st stage bucket. It was demonstrated that trip has no significant impact on initiation of TMF crack near the platform-cooling hole. TBC life at the bucket tip was predicted to be 1810 cycles, or equivalent to 11,000 total hours. This is estimated using the preliminary TBCLIFE model developed by SwRI/EPRI. For the 1st stage bucket, the effect of TGO growth on potential de-lamination or spallation is likely to be less significant compared to the fatigue damage that occurs. Results from the creep analysis reveal that the peak creep strain occurs near the critical crack site, i.e. the platform cooling hole region. The creep life (the time to initiate a creep crack) was predicted to be about 29,000 hours, using a safety factor of three for long-term creep damage. In conjunction with TMF damage, the creep damage may further reduce component life.

The objective of Task 2 is to develop the capability of COATLIFE to handle spallation life prediction for TBCs that are being used in advanced turbines manufactured by major domestic OEMs and to enhance COATLIFE to cover a broader range of McrAlY coatings for oxidation life predicition. The McrAlY coating selected for the evaluation was CT102. The chemical composition of the CT102 is similar to the nominal chemistry of GE's proprietary NiCoCrAlY coating GT-33. Tasks 2.1 and 2.2 deal with coating development for TBC and MCRALY coatings, respectively. The COATLIFE model treats coating degradation mechanisms that are applicable to TBC spallation, and bond coat degradation resulting from loss of aluminum.

Isothermal and cyclic exposure testing of TBC coated specimens at different temperatures has been in progress for several months. The results suggest the thermally grown oxide (TGO) thickness at the TGO/TBC interface increases with increasing exposure time. Additionally, TBC degradation and failure mechanisms were identified including: oxidation, sintering, spallation, and TMF cracking. The results of the isothermal and cyclic exposure testing were used to develop a TBC life model which takes into account each of the identified failure mechanisms. The TBC life model was evaluated for the GTD-111 alloy with a NiCoCrAlY bond coating using the experimental data generated in the program. TBC life values were shown to be in good agreement with the test results.

Under Task 2.2, COATLIFE enhancement for McrAlY coatings, the constants for COATLIFE were determined based on aluminum depletion in the coating. The calculated volume fraction of the remaining beta phase in the coating was also determined to be in good agreement with the measured values of the test specimens exposed a peak temperatures during oxidation testing. COATLIFE algorithms were developed, validated, and implemented into the COATLIFE software for the NiCoCrAlY (CT-102) coating evaluated in Task 2.1.

The objective of Task 3 is to develop inspection technologies sufficient to quantitatively evaluate degradation of service-exposed (and degraded) coatings. Buckets exhibiting various levels of degradation have been acquired for development of the inspection criteria and for destructive analysis.

During this reporting period, eddy current testing and characterization were conducted on one of two 2nd stage 7FA buckets that had undergone 24,000 hours of base-loaded operation with only 40 startups. The eddy current technology was used to demonstrate its capability to provide a qualitative assessment of various coating conditions by separating normal coating, beta phase depletion, and defective coating characteristics associated with TMF. In addition, using a three-layer inversion program, quantitative assessment was made by calculating conductivity values associated with the topcoat, bond coat, and GTD-111 substrate.

Considerable progress has been made over the past several months toward improving the data display by plotting color maps of those calculated parameters, such as normalized impedance values, conductivity values, and coating thickness. The colored contour maps provided good general agreement for locations of high normalized impedance correlated to high conductivity values. The current three-layer inversion program encountered some difficulty separating the topcoat thickness layer reliably from the bond coat thickness layer. This type of assessment would be used to provide quantitative assessment of the coating thickness. Further enhancements are planned for later in 2003 to provide a more accurate coating thickness estimate.

The objective of Task 4 is to validate the predictive capabilities of COATLIFE and the eddy current NDE methodologies (developed in Task 2 and 3 respectively) on service-exposed buckets. This task is slated to begin in November 2004. A TBC coated and service run bucket was obtained during this reported period.

Task 5 work is on hiatus pending the completion of the blade coating metallurgy work (Task 2), NDE work (Task 3), and the final modifications to the COATLIFE software. It is anticipated that work on Task 5 will resume in mid-October 2003. During this reporting period, a software specification was defined for the economic analysis of the hot section buckets.

4.0 TASK 1 REFINEMENT AND VALIDATION OF HSLMP

4.1 Experimental

TMF, creep and TBC cracking/spallation are the primary failure modes of concern for the 1st stage bucket. Platform cracking has been the life limiting issue dictating the repair or replacement intervals for the W501FC 1st stage bucket. Results from steady state aero-thermal and stress analyses suggested that the excessive compressive strain generated at base load might lead to significant thermal fatigue damage for each duty cycle. TMF life is strongly influenced by the total strain range and peak temperature experienced during an operating cycle. EPRI ERA test data from IN738 with RT-122 coating was applied for TMF life prediction (Figure 4.1). Based on these EPRI-derived TMF properties, TMF life (N_f) and strain range ($\Delta\varepsilon$) in % were related by the following equation:

$$N_f = C(\Delta\varepsilon)^n$$

where C = 20.5 and n = -3.93 are applied for IN738 material with a RT-122 coating. Note that a factor of 2 has been applied to the constant C in order to allow for scatter and provide some margin against the affects of the aggressive environment. The transient modes considered when estimating TMF damage included startup, normal shutdown and full load trip.

The premise for achieving long-term reliability for the advanced cooled bucket design is to maintain the core metal temperatures below allowable limits. It has been demonstrated that low surface metal temperatures of W501FC 1st stage bucket are achieved by adopting advanced cooling strategies, relying on lower temperature cooling air, both in conjunction with the application of TBC (Figure 4.2). However, there is growing evidence that localized creep damage can result in creep cracking in a Nickel based super-alloy. Therefore, it is important to calculate creep strain distributions throughout the bucket, especially in high stress regions. A strain-to-failure criterion is used to predict crack initiation at critical locations. A generalized creep equation was derived for IN738 based on regression analysis of test data:

$$\varepsilon(\sigma, T, \text{time}) = 10^{d_3} \cdot \sinh\left(\beta \cdot \frac{time}{time1(\sigma, T)}\right)^{d_4}$$

where

$$time1(\sigma, T) = 10^{LMP(\sigma)/(T+460)-C1}$$

$$LMP(\sigma) = a_3 + a_4 \cdot \log(\sinh(\alpha \cdot \sigma))$$

The generalized creep curve was used for the base metal and bond coat. TBC was not included in the model for creep analysis. Creep damage is assessed based on the following equation:

$$\varepsilon_{cr} = \varepsilon_p + \varepsilon_L$$

$$D_c = \frac{t}{t_{crit}}$$

where

ε_p is the primary creep strain
$\varepsilon_L = d\varepsilon/dt * S_f$ ~ long term creep strain
t_{crit} ~ critical when ε_{cr} reaches creep limit of 1%
$S_f = 3$ ~ safety factor
D_c ~ creep damage

A safety factor of 3 is applied for the long term creep damage to ensure that only one bucket in 10,000 (GE criterion) be allowed to reach a strain-to-failure limit.

A TBC life prediction was also performed based on the preliminary TBCLIFE model developed by EPRI/SwRI. The approach assumes that the spallation of TBC is driven by oxidation-induced strains assisted by thermal cycling fatigue at the TBC/bond interface [1]. The stresses induced by the thermal expansion mismatch between ceramic and metallic layer are greatly influenced by time-at-temperature processes such as oxidation and sintering.

4.2 Results and Discussion

To assess TMF damage, a series of through flow, external gas flow/heat transfer and internal cooling flow/heat transfer calculations were conducted at various time steps during the transient startup, shutdown and trip sequences. Using ANSYS [3], a thermal-mechanical stress calculation was performed subsequent to the transient aero-thermal analysis. Figure 4.3 shows the complete strain-temperature cycles near platform cooling hole for normal shutdown and full load trip cycles. At the inlet of platform cooling hole where cracking occurs, the strain range was calculated to be 0.6% and the corresponding TMF life was predicted to be about 150 cycles in a normal shutdown mode of operation. Temperature near the inlet of platform cooling hole is around 1400ºF at base load. It would appear that excessive compressive stress at base load is the result of highly non-uniform temperature distributions. These are most damaging in terms of the rate of consumption of the TMF life. A comparable level of strain range was calculated at the interface between the TBC and bond coat, above the inlet of platform cooling hole. The interface temperature at steady state is about 1540ºF. It is very likely that once a TMF crack is initiated, either at the inlet of cooling hole or at the bond coat underneath the TBC, a through-crack across the platform thickness is immediately formed. The platform through-thickness crack becomes the life-limiting factor that dictates the replacement and repair interval of the 1st stage bucket.

As shown in Figure 4.3, the effect of a unit trip on TMF life in terms of the platform cracking is insignificant. At the leading edge of the airfoil, the effect of a unit trip on TMF damage is more pronounced (Figure 4.4). The tensile stress generated during the trip is increased and the corresponding TMF life is reduced. The transient thermal response at the platform is not as severe as

the leading edge, where the edges respond faster, cool more quickly than the bulk section and thereby result in a tensile strain. In addition, a TBC tends to reduce the transient thermal response and moderate the transient stresses. The TMF damage at platform is most critical and it has been demonstrated that trip has no substantial impact on crack initiation. A factor of 20 implied by OEM appears to be overly conservative in terms of providing an estimation of the damage at the platform caused by a full load trip.

W501FC 1st stage bucket utilizes commercially available material IN738 for a base material. More exotic materials, such as GTD111 (a derivative of Rene 80), have been adopted by GE for the same class of rotating buckets. It has been reported by the OEM that GTD111 has 50% improved creep strength over U500. Based on stress rupture test data, a parametric study was performed to compare creep strength and temperature advantage between IN738 and GTD111 materials. As shown in Figure 4.5, GTD111EA has approximately a 70º F temperature advantage over IN738 for the stresses near 30~50 ksi. The temperature advantage is reduced significantly when stresses are below 10 ksi. GTD111DS has a much higher temperature advantage over IN738 in a lower stress range. At stress levels of 40 ksi, GTD111DS also has a similar temperature advantage over IN738 of 70º F. To account for the relatively low creep strength of IN738 material (compared to GTD111), additional cooling is required to maintain a sufficient or similar temperature margin. The temperature of cooling air supplied to the W501FC 1st stage bucket is about 470º F, or substantially lower than 730º F seen for the 7FA of similar design. Adoption of a TBC would further reduce temperature levels in the metal. However, high local thermal stress might be produced as a result of excessive temperature gradients. This is believed to explain why severe platform cracking was experienced by W501FC 1st stage bucket.

Figure 4.6 shows the creep strain distribution after 24,000 hours. The peak creep strain was predicted near the platform cooling hole where cracking occurs. The accumulated creep strain approached 1% after 24,000 hours. The time history of accumulated strain shows a significant rate of primary creep strain in the early stages of use and a very mild creep strain rate over the longer term. This is caused by the thermal stress that is the main driving force of the creep damage. The creep life (the point where creep might initiate cracks) was predicted to be about 29,000 hours. This estimate used a safety factor of three for long term creep damage (Figure 4.7). In conjunction with TMF damage, it is concluded that the creep damage may further reduce the life of this component.

The interface temperature between TBC and bond coat is generally low in the airfoil, as shown in Figure 4.2, and the peak interface temperature remains below 1500º F at airfoil mid-section. The leading edge on the suction side at the bucket tip appears to be the hottest spot, based on the results of the aero-thermal analysis. The peak temperature at the bond/TBC interface was calculated to be around 1810ºF. For a cycle time of 6 hours per cycle, which is typical for a peaking machine, the TBC life was calculated to be about 1810 cycles, or equivalent to 11,000 total hours. A 10 Gpa fatigue strength coefficient was assumed in the analysis. Sensitivity studies show that the TBC life will be reduced to 380 cycles, or equivalent to 2,280 hours when a fatigue strength coefficient of 5 Gpa (reduced by 50%) is applied. The damage is primarily attributed to fatigue under this temperature range. The effect of TGO growth on potential de-lamination or spallation appears less significant as compared to the fatigue damage. Further calibration of the model is required to refine the analysis.

Figure 4.1 – EPRI TMF Life Properties

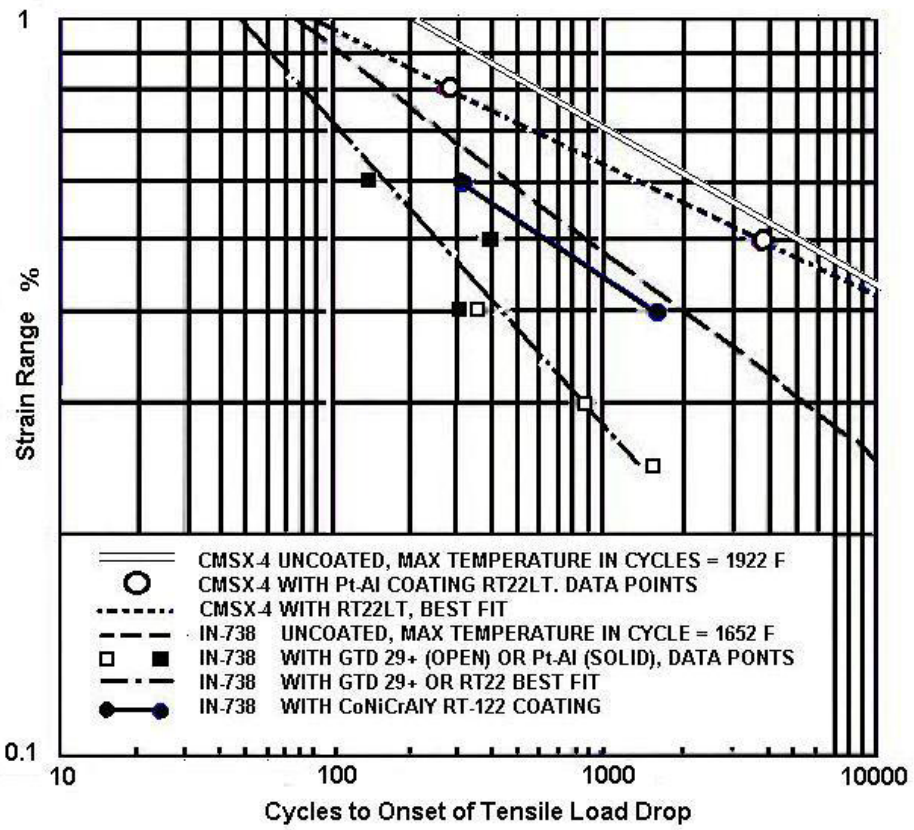

Figure 4.2 – Temperature Distributions in the TBC system at 50% Bucket Heigh

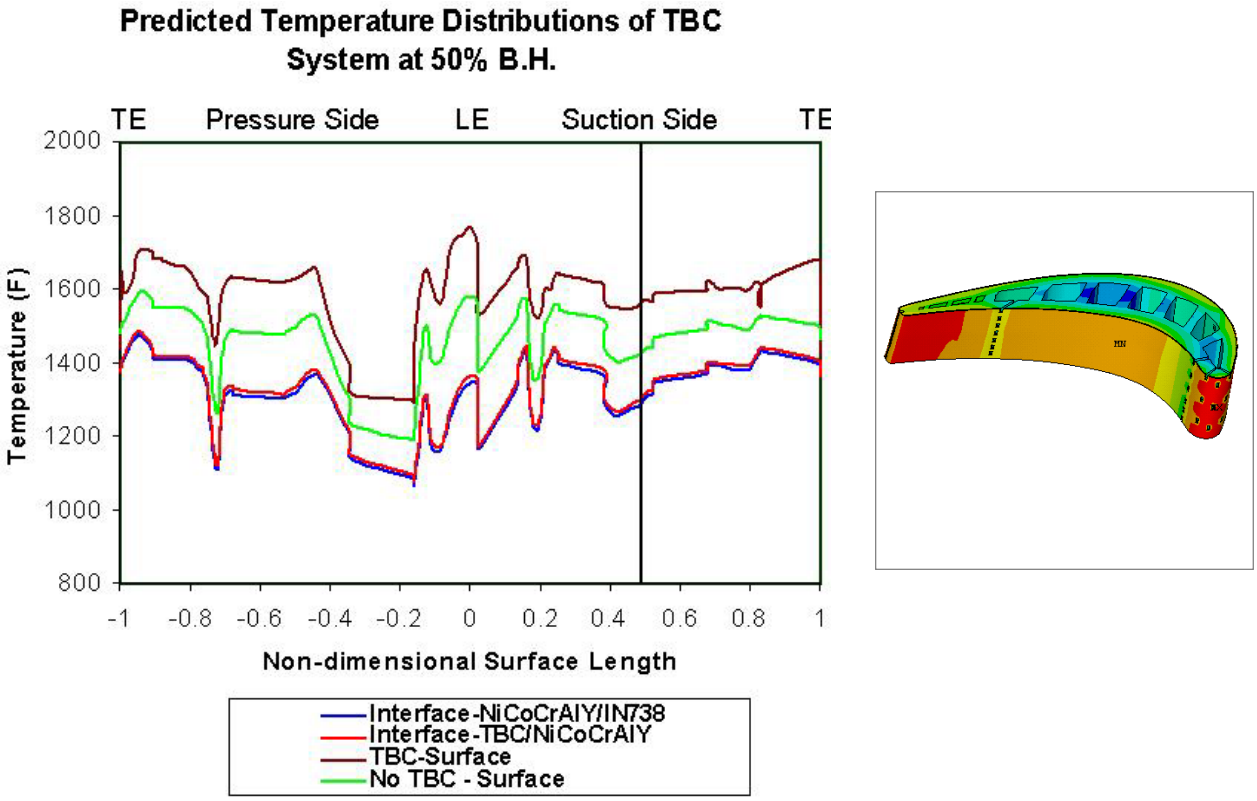

Figure 4.3 – TMF Strain-Temperature Cycle – Platform Cooling Hole

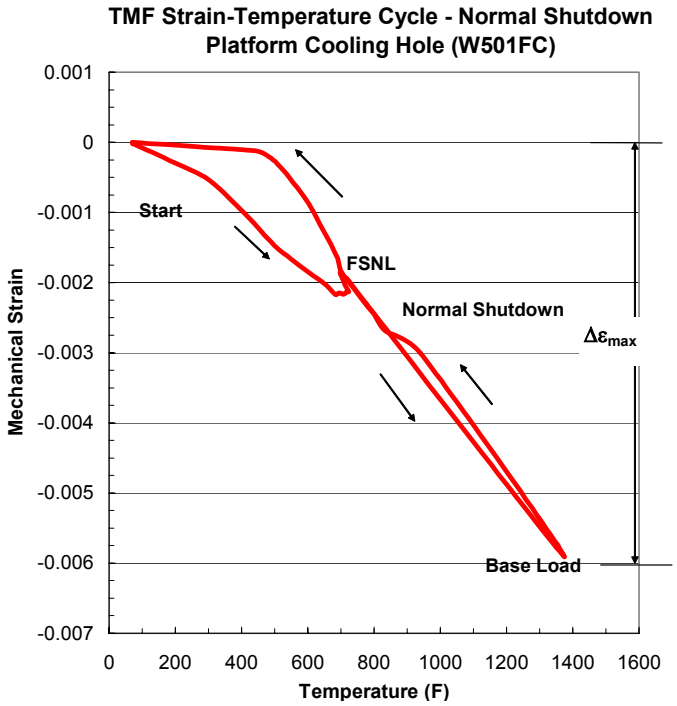

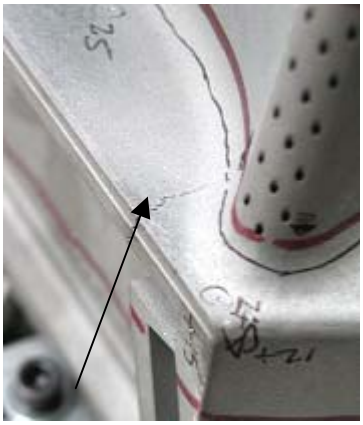

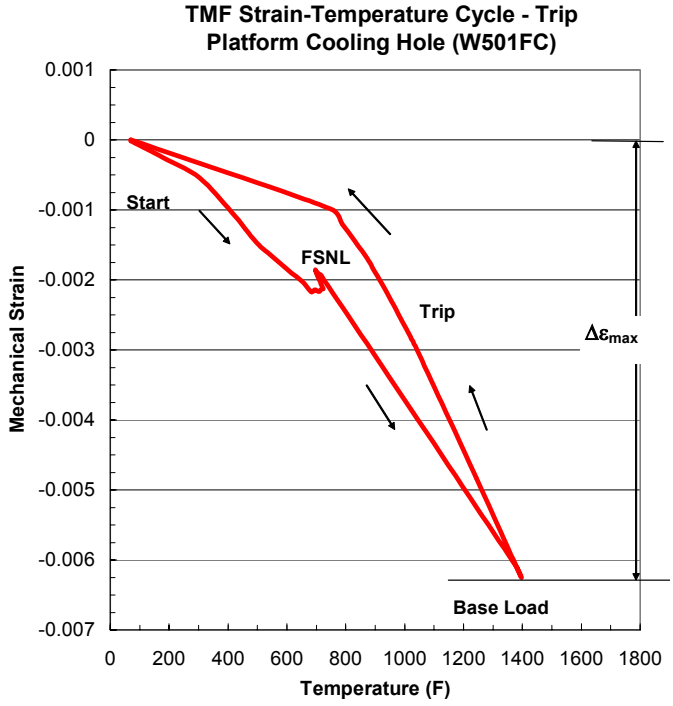

Figure 4.4 – TMF Strain-Temperature Cycle – LE at 50% Bucket Height

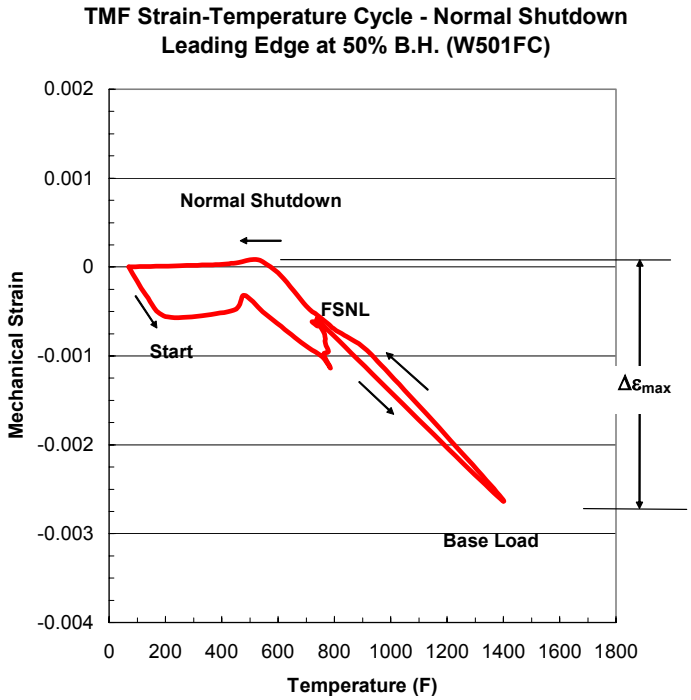

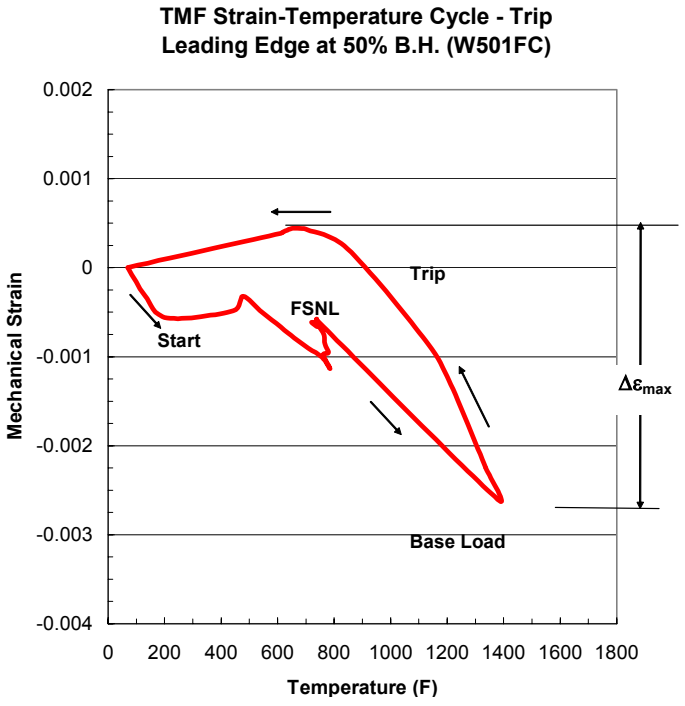

Figure 4.5 – Creep Advantage Curve – GTD111 vs. IN738

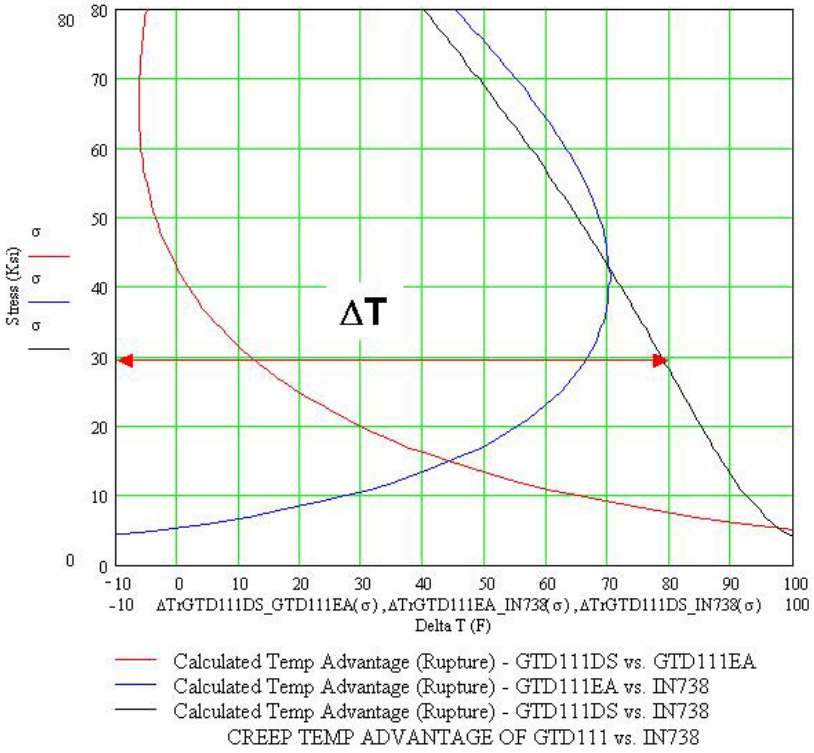

Figure 4.6 – Creep Strain Distributions after 24,000 hours

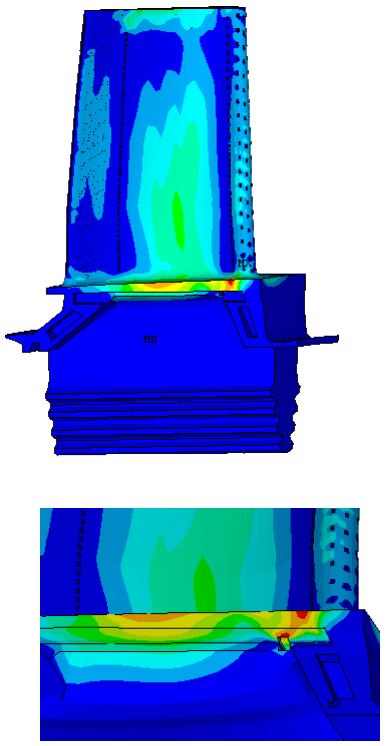

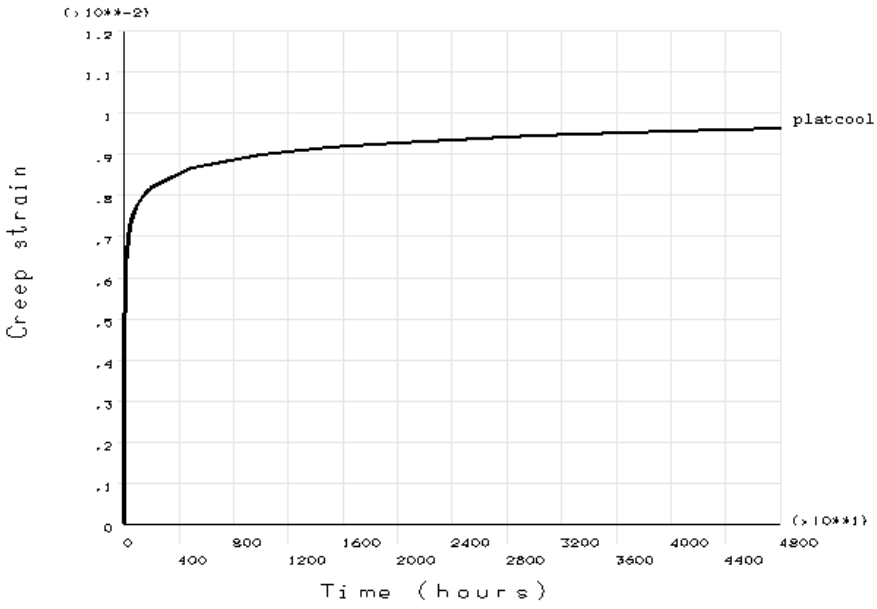

Figure 4.7 – Predicted Time History of Creep Damage

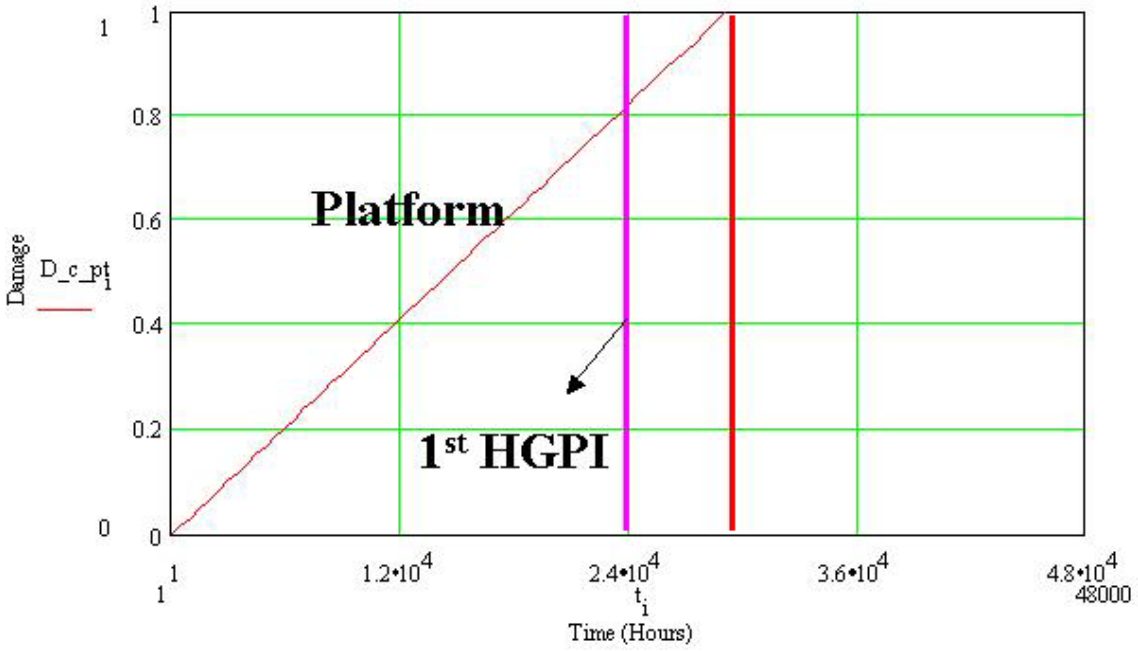

4.3 Conclusions—Task 1 Refinement & Validation of HSLMP

- It appears that platform cracking is the primary life limiting issue that dictates the repair and replacement interval of the W501FC 1st stage bucket. TMF is the predominant damage mechanism that governs the reliability of the buckets operated in a cyclic mode. It was found that an excessive compressive stress occuring at base load is a result of highly non-uniform temperature distributions. These are most damaging in terms of the consumption of TMF life. At the location where platform cracking has occured, the strain range was calculated to be 0.6% and the corresponding TMF life was predicted to be about 150 cycles for a normal shutdown mode. Substantial fatigue cracking in the platform might lead to premature retirement of the blade long before the 1st HGPI of 800 cycles.

- It was demonstrated that trip has no substantial impact on initiation of TMF crack near the platform cooling hole. The effect of a unit trip on TMF damage is more pronounced at the leading edge of airfoil. The transient thermal response at the platform is not as severe as the leading edge, where the faster edges cool more quickly than the bulk section, resulting in a tensile strain. In addition, TBC tends to reduce the transient thermal response and moderate the transient stresses. A factor of 20 applied by the OEM is considered overly conservative for the estimation of damage at platform caused by a full load unit trip.

- Creep may also contribute to the platform cracking. Results from the creep analysis reveal that the peak creep strain occurs near the critical crack site, near the platform cooling hole region. The creep life for initiating a creep crack was predicted to be about 29,000 hours. In conjunction with TMF damage, the creep damage may further reduce component life.

- The TBC life at bucket tip was predicted to be about 1810 cycles, or equivalent to 11,000 total hours using the preliminary TBCLIFE model developed by SwRI/EPRI. For the 1st stage bucket, the effect of TGO growth on potential de-lamination or spallation appears less significant as compared to fatigue damage. Bond coat oxidation may be an issue in long-term performance for machines operated as base load providers. Overall, quality issues, foreign object damage and erosion might have more impact on the TBC life for the 1st stage bucket.

5.0 TASK 2: COATLIFE FOR ADVANCED METALLIC COATINGS AND TBCs

5.1 Task 2.1 Thermal Barrier Coatings

5.1A Experimental Procedures

Materials and Coatings

Three shank sections of GTD-111 DS blades and three shank sections of IN-738 blades retired from Frame 5002 engines were procured for machining test coupons. The shank sections operate at a much lower temperature than the airfoil section of a blade and, as a result, the material at the shank section is not expected to degrade during service. The structure and properties of the material at the shank section represent the initial, as heat-treated condition.

Compositional measurements were made at selected locations on the GTD-111 and IN-738 blade shank sections using energy dispersive X-ray spectroscopy (EDS). The composition of the blade materials is given in Table 5.1.

Table 5.1. Chemical composition of GTD-111 and IN-738 test materials (wt. %).

Blade	Al	Ti	Cr	Co	Mo	Nb	Ta	W	Ni
GTD-111	3.2	5.2	14.4	9.2	2.1	—	4.0	3.2	Bal
IN-738	3.8	3.6	16.0	8.3	1.9	1.1	2.1	2.2	Bal

About 150 cylindrical specimens (0.36 inch diameter and 1.5 inches long) were removed from the GTD-111 and IN-738 blade shank sections using an electro-discharge machining process. The specimens were ground and polished to remove the recast layer. Turbine Airfoils, Coatings, and Repairs (TACR) applied bond and yttria stabilized zirconia coatings. A low-pressure plasma spray process (LPPS) was used to apply NiCoCrAlY (CT102) coating to all specimens. The composition of the powder is given in Table 5.2. The composition of the powder is comparable to the nominal chemistry of GE's proprietary coating GT33. After application of the coating all specimens were given a vacuum diffusion treatment at 1121°C (2050°F) for two hours. An approximately 10 μm thick layer of platinum was applied by electroplating on half of the NiCoCrAlY coated specimens. The Pt plated NiCoCrAlY was selected because Siemens Westinghouse uses the platinum-plated CT102 as a bond coating for TBC-coated parts of advanced turbines. Following electroplating, the specimens were given a vacuum diffusion heat treatment at 1121°C (2050°F) for two hours. All CT102 and platinum-plated CT102 specimens were then given an aging treatment at 843°C (1550°F) for 24 hours prior to the application of the top ceramic coating, a standard yttria stabilized zirconia, by using an air plasma spray (APS) process. The chemical composition of the ceramic coating powder is given in Table 5.3.

Table 5.2. Chemical composition of CT102 bond coating powder (wt%).

Al	Co	Cr	Ni	Y
8.0	Balance	21.0	32.0	0.5

Table 5.3. Chemical composition of ceramic coating powder (wt.%).

Al_2O_3	Fe_2O_3	SiO_2	TiO_2	Y_2O_3	HfO_2	ZrO_2
0.13	0.02	0.27	0.09	7.69	1.85	Balance

Isothermal Tests

Multiple TBC-coated GTD-111 and IN-738 specimens with two different bond coatings are being aged in three different furnaces, which are maintained at three temperatures: 1010°C (1850°F), 1038°C (1900°F), and 1066°C (1950°F). One specimen from each substrate/coating system is being removed at predetermined intervals for metallurgical evaluation.

Cyclic Exposure Tests

Cyclic exposure testing of coated specimens was conducted at two peak temperatures of 1950°F (1066°C) and 1850°F (1010°C). The coated specimens were cycled between the peak and room temperatures. The thermal cycle consisted of holding the specimens at the peak temperature for 55 minutes and then air cooled for five minutes.

5.1B Results and Discussion

Isothermal Exposure Testing

Isothermal exposure testing of the tbc–coated specimens at 1010°c (1850°f), 1038°C (1900°F), and 1066°C (1950°F) has been initiated. The specimens have been exposed for 10,000 hours at 1010°C (1850°F), 6000 hours at 1038°C (1900°F), and for 4079 hours at 1066°C (1950°F) to date. Examination of these specimens revealed no external tbc surface cracking on the specimens exposed at 1010°C (1850°F) and 1038°C (1900°F). The condition of the specimens after 9850 hours exposure at 1850°F (1010°C) is shown in Figure 5.1.

Figure 5.1: Condition of Coated Specimens after 9855 hours Exposure 1850°F (1010°C). Note that there ware no visible cracks

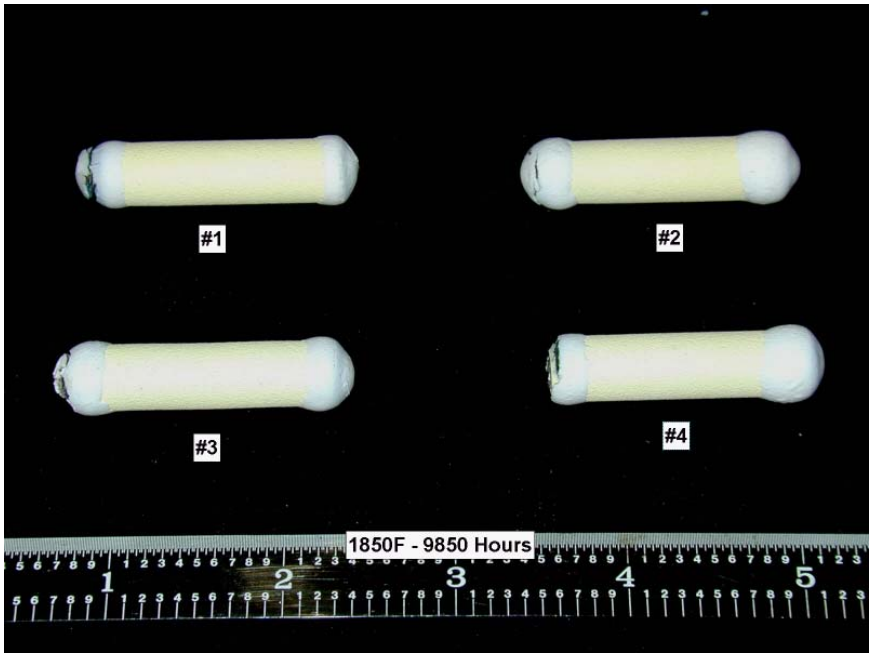

Cracks and/or TBC spallation were seen on the specimens exposed at 1066°C (1950°F). Cracking time varied for different base metal/bond coat/TBC systems. Time to crack TBC for different systems is given in Table 5.4. Typical morphology of cracking spallation of the TBC on the specimens are illustrated in Figure 5.2

Table 5.4: TBC cracking and/or Spallation Time after isothermal exposure at 1066°C (1950°F)

System ID	Base Metal	Bond Coating	Time to Crack or Spall TBC, hours
1	GTD 111	NiCoCrAlY	2925
2	IN 738	NiCoCrAlY	2785
2	IN 738	NiCoCrAlY	3517
3	GTD 111	NiCoCrAlY+Pt	3767
4	IN 738	NiCoCrAlY+Pt	4079

Figure 5.2: Photographs of coated specimens after exposure at 1066°C (1950°F). Arrows point to the cracks.

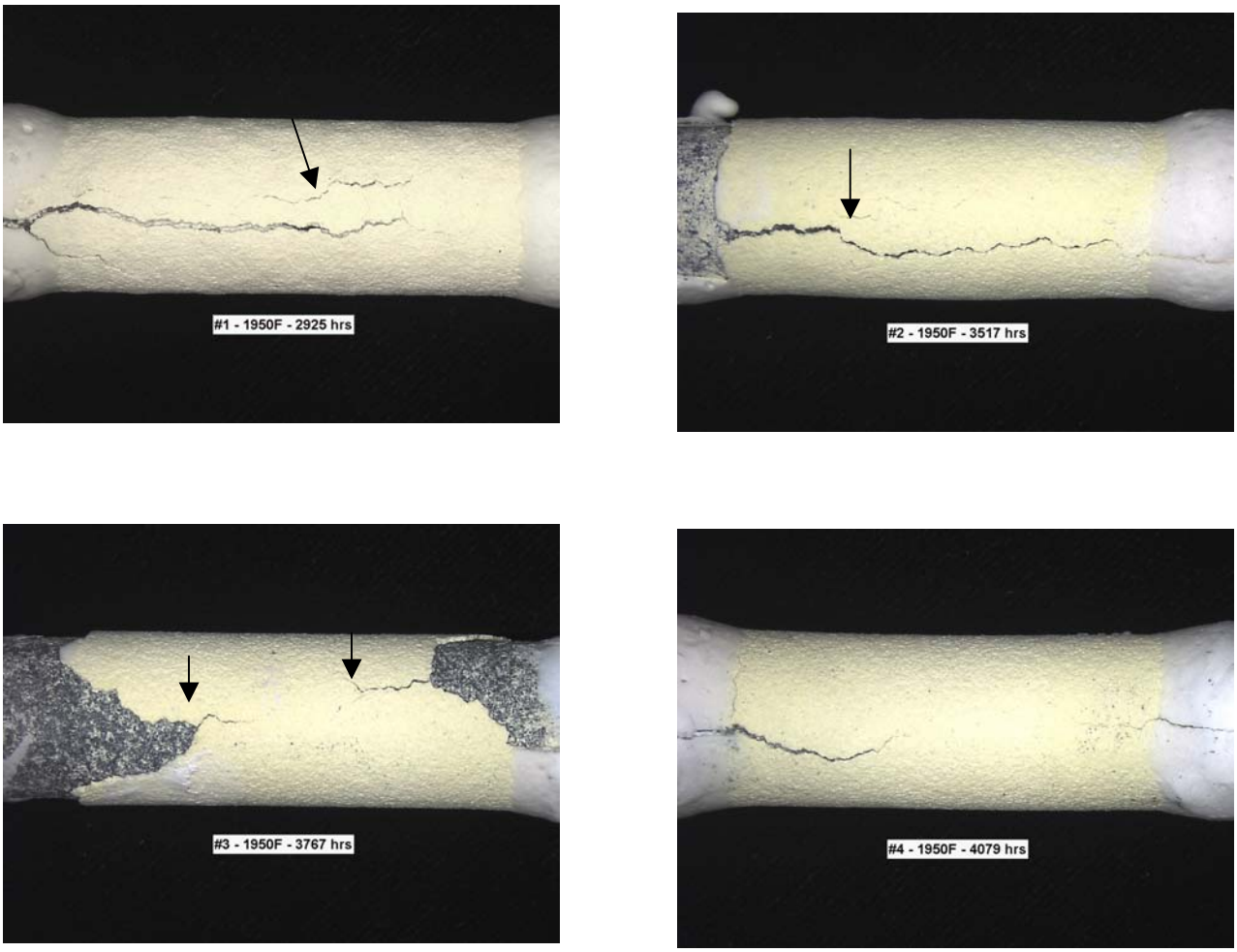

Cyclic Exposure Testing

Cyclic exposure testing of the TBC–coated specimens at the peak temperature of 1066°C (1950°F) was completed. The test results are shown in Table 5.5. The preliminary results show that the durability of TBC depends on the composition of the bond coating and the base material. Platinum plating over the NiCoCrAlY coating on both GTD 111 and IN 738 seems to increase life of the TBC. The TBC on the platinum plated NiCoCrAlY bond coated IN 738 specimens exhibited the highest resistance to cracking and/or spallation.

Table 5.5: Thermal cycling between 1066ºC (1950ºF) and room temperature test results

System ID	Base Metal	Bond Coating	Cycles to Crack or Spall TBC
1-1	GTD 111	NiCoCrAlY	863
1-2	GTD 111	NiCoCrAlY	760
1-3	GTD 111	NiCoCrAlY	1129
2-1	IN 738	NiCoCrAlY	793
2-2	IN 738	NiCoCrAlY	836
2-3	IN 738	NiCoCrAlY	890
3-1	GTD 111	NiCoCrAlY+Pt	1258
3-2	GTD 111	NiCoCrAlY+Pt	966
3-3	GTD 111	NiCoCrAlY+Pt	914
4-1	IN 738	NiCoCrAlY+Pt	1565
4-2	IN 738	NiCoCrAlY+Pt	1823

Cyclic exposure testing of the TBC–coated specimens at the peak temperature of 1010°C (1850°F) has been in progress. These specimens have been exposed for about 1800 one-hour thermal cycles to date. No cracking of TBC was observed on any of these specimens.

Cyclic exposure testing with 24 hours hold time at the peak temperature of 1066°C (1950°F) has been initiated and the specimens exposed for about 25 cycles to date.

MICROSTRUCTURE OF EXPOSED SPECIMENS

Metallurgical mounts were prepared from the samples removed after exposure at 1010°C (1850°F), 1038°C (1900°F), and 1066°C (1950°F) for different times. The TGO scale thickness as a function of time and temperature was determined for the GTD 111 alloy with NiCoCrAlY bond coating. The results are shown in Table 5.6. Typical morphology of the TGO scale is shown in Figures 5.3 and 5.4. It can be seen from the results that the TGO scale thickness increased with exposure time and temperature. These results are used to evaluate the TBC life model.

Table 5.6: Influence of exposure temperature and time on thermally grown oxide (TGO) scale thickness on TBC coated specimens

SYSTEM ID	BASE MATERIAL	BOND COATING	EXP. TEMP ºC (ºF)	EXP. TIME HOURS	AVE. TGO THICKNESS, MM
1	**GTD-111**	**NICOCRALY**	**1066 (1950)**	**1510**	**11.3**
				2025	**13.6**
				2785	**17.8**
				2925	**19.4**
			1038 (1900)	**1005**	**8.8**
				2015	**12.5**
				4510	**17.5**
			1010 (1850)	**2015**	**9.8**
				5015	**12.0**
				8155	**16.6**
				9850	**18.9**

Figure 5.3 Optical micrographs showing variation of TGO thickness (a) after 1510 and b) after 2785 hours exposure at 1066°C (1950°F)

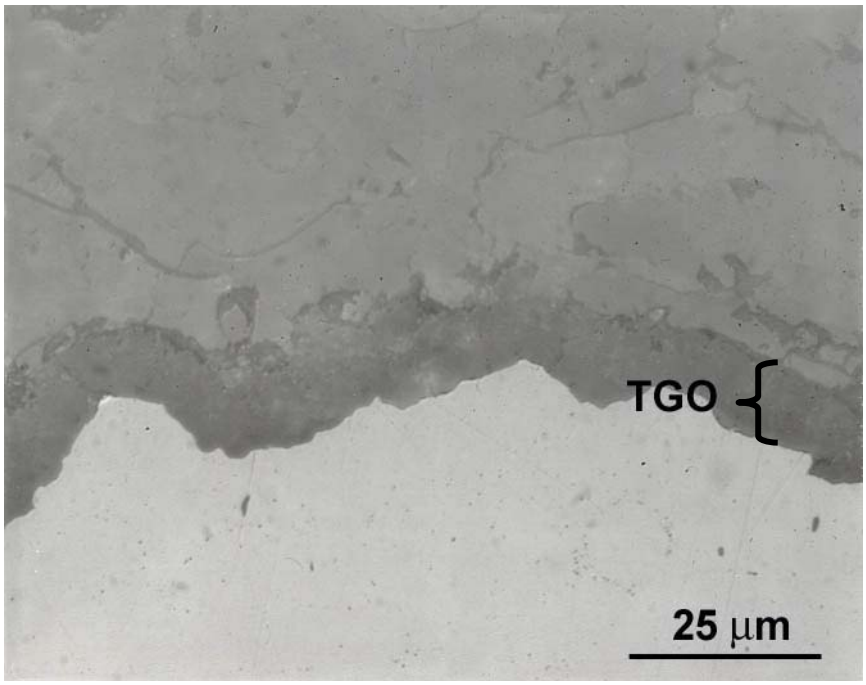

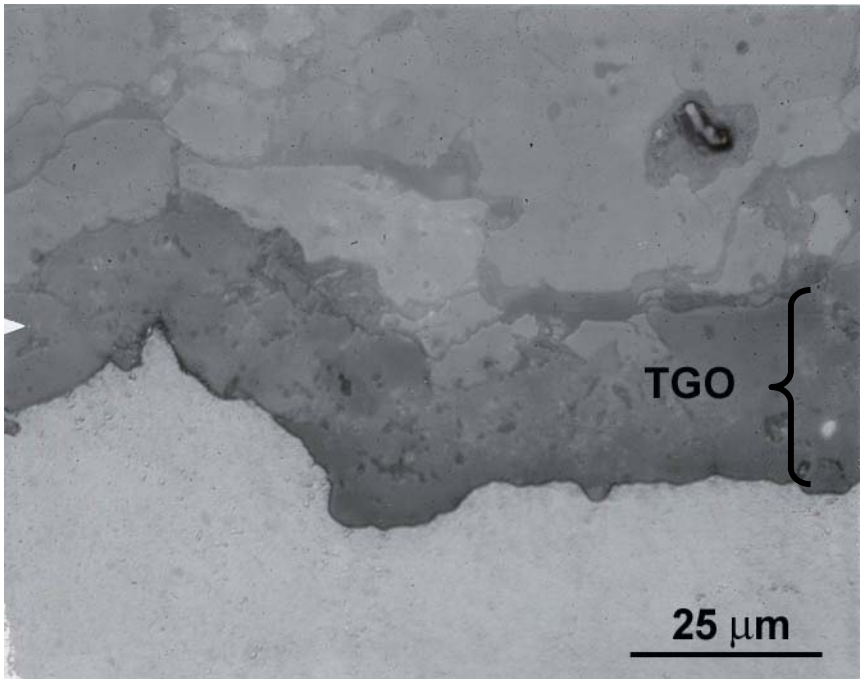

Figure 5.4 Optical micrographs showing variation of TGO thickness (a) after 1510 and b) after 2785 hours exposure at 1010°C (1850°F)

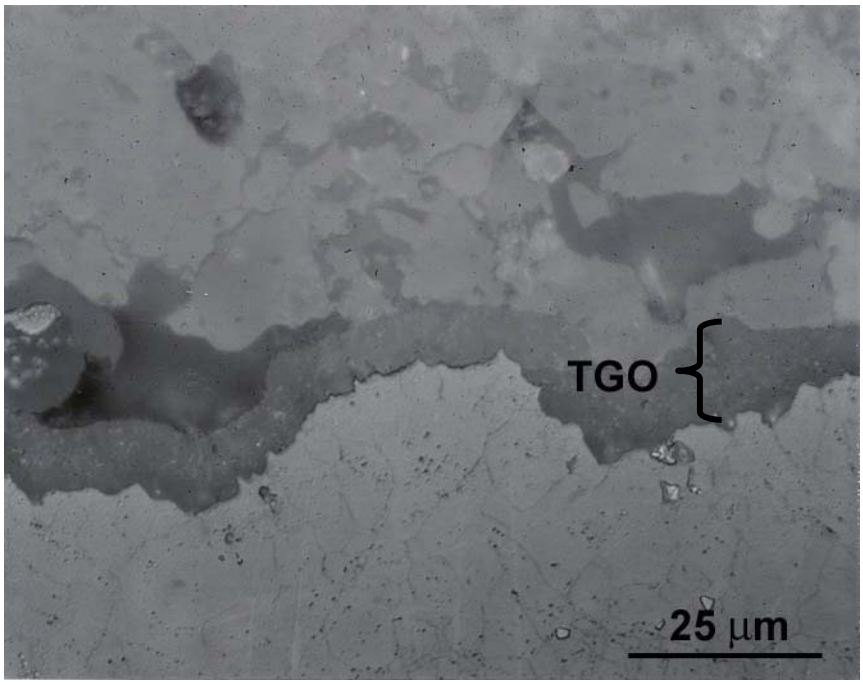

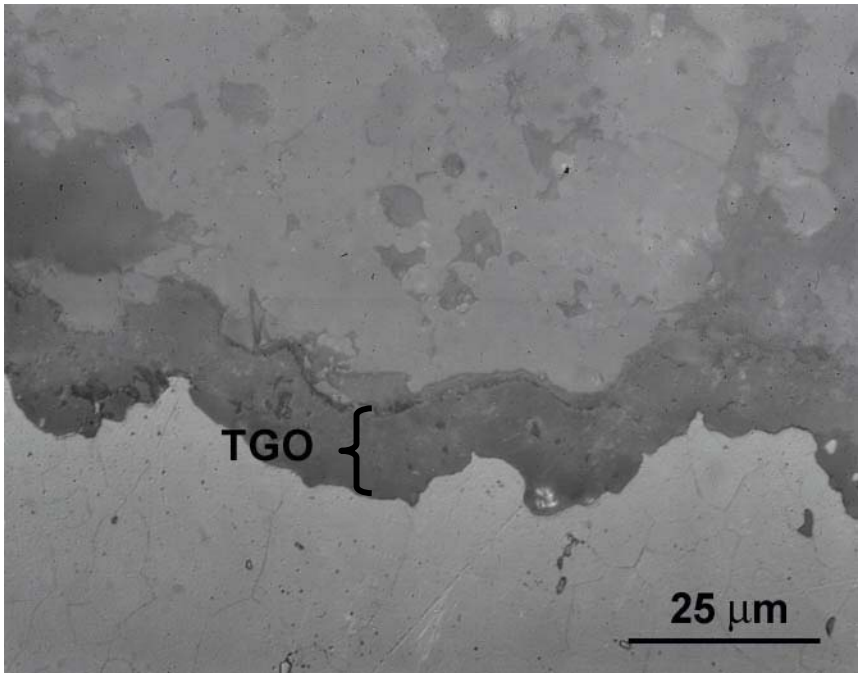

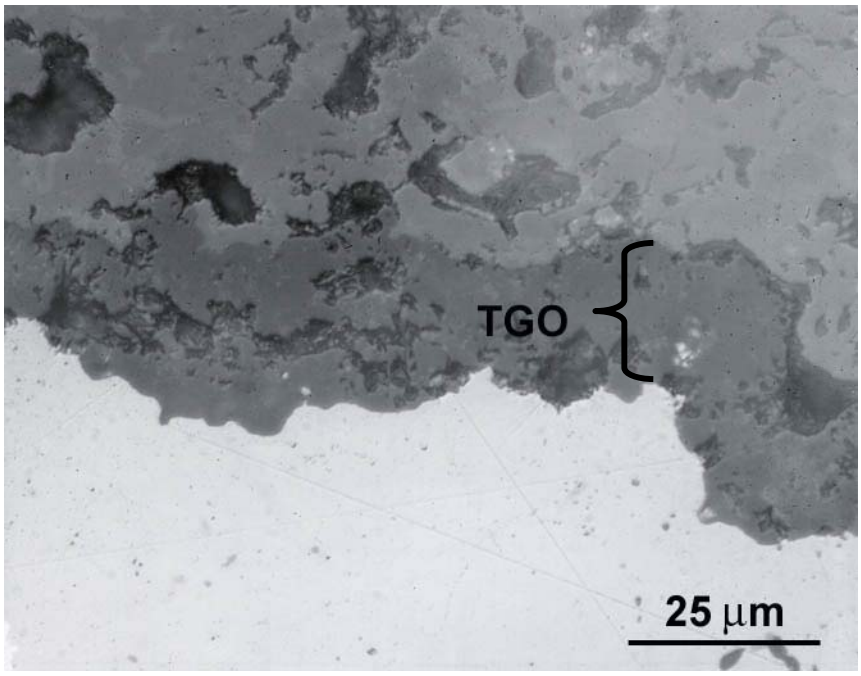

5.1C TBC Life Algorithm Development

The oxidation kinetics of the APS TBC/NiCoCrAlY bond coat was characterized using a parabolic rate equation for describing the TGO thickness, δ, as a function of time, t, of thermal exposure. The parabolic rate constant was obtained by plotting the TGO thickness as a function of $t^{1/2}$. Linear regression of the experimental data, provided the value of the parabolic rate constant, k_p, at a given temperature, T. Comparison of the calculated and measured oxide thickness were made at 1950F (1066C) and 1850F (1010°C). Based on the time at failure, the critical TGO thickness at TBC failure was determined to be about 20 μm

The oxidation kinetic constants and the critical TGO thickness were utilized in conjunction with the TBC life model to compute the number of start-up cycles as a function of cycle time. A comparison of the calculated and measured TBC lives for APS TBC tested at a peak temperature of 1066°C (1950°F). Excellent agreement was obtained because the critical TGO thickness was derived from the same set of experimental data. The TBC model was also used to predict the coating life diagram for 1010°C (1850°F). Both the cyclic and isothermal oxidation tests for 1010°C (1850°F) are still in progress without TBC cracking or failure. A comparison of model predictions and experimental data will be made as soon as the experimental data become available. Fine-tuning of the model constants may also be made, depending on the agreement between the model predictions and the experimental data.

5.1.D Task 3A Conclusions--Thermal Barrier Coatings

- Isothermal and cyclic exposure testing of TBC coated specimens at different temperatures has been in progress. The results showed that the TGO thickness at the TGO/TBC interface increases with increasing exposure time.
- TBC degradation and failure mechanisms included, oxidation sintering, spallation, and TMF cracking. Considering all pertinent failure mechanisms, a preliminary TBC lifing model was developed.
- The TBC life model was evaluated for GTD 111 alloy with NiCoCrAlY bond coating using the experimental data generated in this program. The calculated TBC life values are in good agreement with the test results

Task 5.2 MCrAlY Coating

Task 5.2A Experimental Procedures

Materials and Coatings

Flat rectangular specimens were machined from the shank sections of GTD-111 buckets using an electro-discharge machining process for thermal cycling tests at two peak temperatures. TACR applied CT102 coating on these specimens using an LPPS process. Following application of the coating, the specimens were given a vacuum diffusion heat treatment at 1121°C (2050°F) for two hours and an aging treatment at 843°C (1550°F) for 24 hours.

Metallurgical Evaluation of Coated Specimens

For metallographic evaluation, a transverse section was removed from coated specimens. The sections were mounted in a conductive mounting media, polished using standard metallographic techniques, and examined under optical and scanning electron microscopes to characterize the coating structure and to determine the chemical composition of the coating either in the as-coated or post-exposed condition. The composition of the phases in the coating was determined using Energy Dispersive Spectroscopy (EDS) and the volume fraction of β-phase in the coating was determined using quantitative metallographic techniques.

Cyclic Oxidation

Cyclic oxidation tests were conducted using a facility designed and fabricated at Southwest Research Institute. The test facility consists of a furnace, a forced air cooling system, a coated superalloy frame for suspending test specimens, and a computer controlled moving arm that transfers specimens in and out of the furnace and to the cooling system. For cyclic oxidation testing, coated specimens were inserted into the furnace, which was maintained at a desired peak temperature and held at that temperature for 55 minutes prior to moving them into the cooling system. Following cooling the

specimens for 5 minutes, to room temperature, the specimens were then reinserted back into the furnace. The tests were interrupted at predetermined intervals to weigh the specimens.

5.2B Results and Discussion

Cyclic Oxidation

Cyclic oxidation tests were conducted at two peak temperatures, 1010C (1850°F) and 1060°C (1950°F). At both temperatures, weight change was determined as a function of thermal cycles. The volume of fraction of beta phase and aluminum content in the coating were also determined as a function of thermal cycles. These results are used to determine the constants of the COATLIFE model and to develop COATLIFE algorithm. Due to the large volume of data and graphics, this information has not been included herein.

5.2C Coating Life Algorithm Development

The model constants for NiCoCrAlY at 1010°C were finalized based on the cyclic oxidation data generated in this program. Weight changes were measured and computed against these predictions by the model. The observed weight changes are larger than those predicted by the model after 1000-2000 thermal cycles. In both cases, the computed values of the Al content and the volume fraction of β phase are lower than the experimental data when the thermal cycle exceeds 2000. This finding indicates that Al and β-phase depletion occur at lower rates than model prediction. Chemical analyses of oxides formed on the surface specimens indicated that the oxide layer contained a mixture of alumina, yttria, and chromia when the number of thermal cycle exceeded 2000 cycles. In addition, oxidation pits, which are indicative of localized oxidation, were observed in specimens after 3500 thermal cycles. The discrepancy between model prediction and experimental data was therefore due to the absence of a continuous alimina scale on the oxidized surfaces.

Coating Life Prediction Based On NDE Input

A set of procedures were developed for computing the remaining life of an MCrAlY using NDE data as input. One life equation was developed on the basis of linear depletion of the Al content, while another was developed on the basis of linear consumption of the β-phase in the coating. Both assumptions are currently used in COATLIFE for summing up damage accumulation under variable temperatures. For linear depletion of Al content, the remaining life, RL(T), of an MCrAlY at temperature T can be computed based on the current Al content via the expression given by

$$RL(T) = \left[\frac{X_{Al} - X^*_{Al}}{X_{Al}(0) - X^*_{Al}} \right] N_f(T) \qquad (1)$$

where X_{Al} is the current level of Al content determined by NDE, $X_{Al}(0)$ is the initial Al content in the pristine coating, X^*_{Al} is the critical Al content, and $N_f(T)$ is the coating life for temperature T. For linear depletion of $\tilde{\beta}$-phase, RL(T) is given by

$$RL(T) = \left[\frac{V_\beta}{V_\beta(0)} \right] N_f(T) \qquad (2)$$

where V_β is the volume percent of β and V_β (0) is the initial volume percent of β in the pristine coating.

COATING LIFE DIAGRAMS FOR NICOCRALY

Coating life diagrams for GT33 were computed for various temperatures ranging from 1500°F (816°C) to 1950°F (1066°C) at 50°F (28°C) increments. The coating life diagrams were parameterized in terms of a two-parameter power-law whose coefficients are temperature dependent. These temperature-dependent coefficients were expressed as a function of temperature and the results were incorporated into COATLIFE Version 3.0.

THERMOMECHANICAL FATIGUE LIFE (TMF) RELATION FOR NICOCRALY

Thermomechanical fatigue life data developed in this program were utilized to develop the TMF life relation for NiCoCrAlY coatings on GTD-111DS. The thermomechanical fatigue (TMF) model utilized in this program has the form given by

$$\Delta\varepsilon_m = CN_f^{-a} \tag{3}$$

where $\Delta\varepsilon_m$ is the mechanical strain range, N_f is the cycle-to-failure, C is the fatigue ductility coefficient, and α is the fatigue life exponent. Material constants in the TMF model, which are C and α, were evaluated by plotting the experimental data in a log-log plot of mechanical strain range versus cycles-to-failure. Least-square regression analysis was then performed to obtain the values of C and α for a particular coating/substrate combination. The value of C was then reduced to give the minimum coating life in the data set. The adjustment in the C value was necessary because of scatter in the TMF data. Finally, the C value was further reduced to that corresponding to 1/2 of the minimum life. This was done so that the predicted TMF life would be conservative. The TMF life equations and experimental data for NiCoCrAlY/GTD-111DS were evaluated. Also, a comparison of the TMF life equation for NiCoCrAlY/GTD-111DS against those for NiCoCrAlY+/GTD-111DS and NiCoCrAlY/IN-738 was examined.

COATLIFE — VERSION 3.5

Aluminium oxidation-life and TMF life equations for NiCoCrAlY coating on GTD-111DS were incorporated into COATLIFE 3.0. In addition, the graphical-user interface (GUI) for COATLIFE 3.0 was revised to allow NDE input of Al content and volume percents of beta phase and the computation of remaining coating life using the NDE data. Because of these additions, COATLIFE Version 3.0 was upgraded to Version 3.5. Figure 5.5 shows the revised GUI of COATLIFE Version 3.5 that includes columns for temperature, cycle time, and number of start-up cycles, as well as additional columns for NDE input of Al content and volume percent of beta phase. The radio-button under each of these columns allows the user to select the mode of data input. The predicted coating life obtained from the selected data input is shown under the "Failure Cycles" column at the right of the GUI.

Figure 5.5. Revised graphical user interface (GUI) of COATLIFE that allows data input in terms of number of start-up cycles, as well as NDE input of Al content and volume percent of β-phase for remaining life calculation.

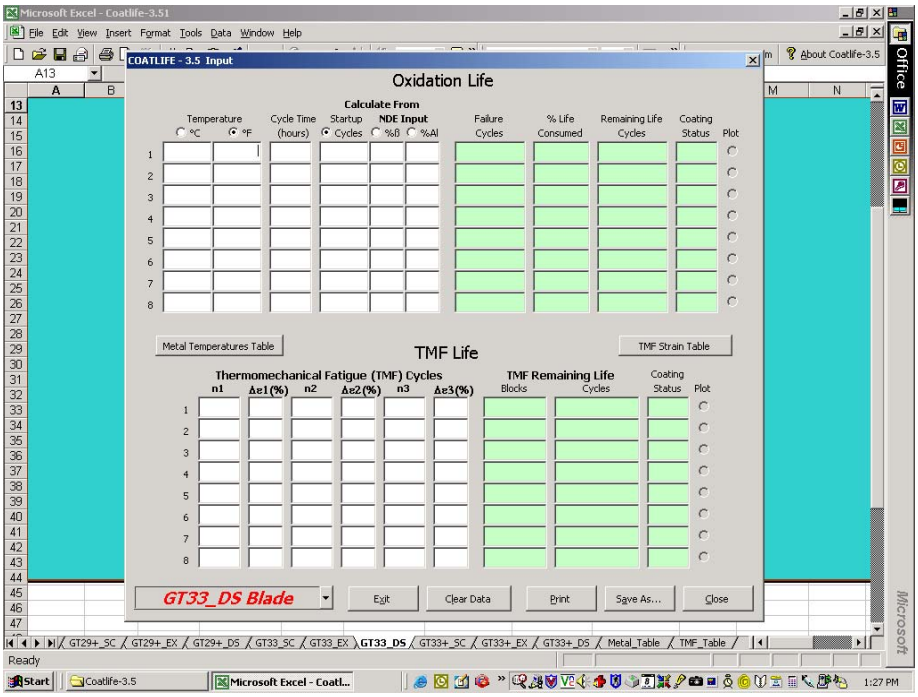

As an illustration, Figure 5.6 shows the data input for lifing GT33/GTD-111DS on the basis of the number of start-up cycles for 24-hour thermal cycling at a peak temperature of 1800°F (982°C). The computed coating life (failure cycles), percent life consumed, the remaining life, and the coating status are shown under the corresponding columns at the right of the GUI, while the predicted TMF data input and results are shown at the lower portion of the GUI. The coating life diagram for

GT33/GTD-111DS for 1800°F (982°C) is presented in Figure 5.7, which shows the current coating condition as a pink square symbol, the Al oxidation life boundary as a red line and the TMF life boundary as a pink horizontal line. For the conditions examined, the coating is currently safe since the accumulated number of start-up cycles is well below the Al oxidation life and the TMF life boundaries.

Figure 5.6. Graphical-user Interface shows data input and predicted coating life for GT33/GTD-111DS subjected to thermal cycling at a peak temperature of 1800°F (982°C) and a cycle time of 24 hours for 200 start-up cycles. The TMF strain ranges are 200 cycles at 0.55%. The predicted oxidation life, percent life consumed, and the remaining life are 728.08 cycles (or 17,474 hours), 27.47%, and 528.08 cycles, respectively, while the predicted remaining TMF life is 529.29 cycles.

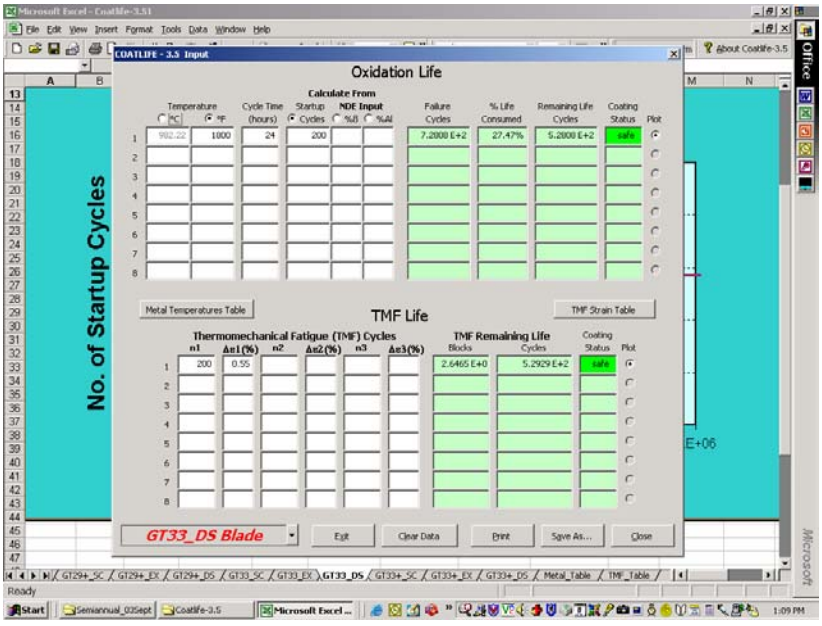

Figure 5.7. Coating life diagram predicted for GT33/GTD-111DS at 1800°F (982°C).

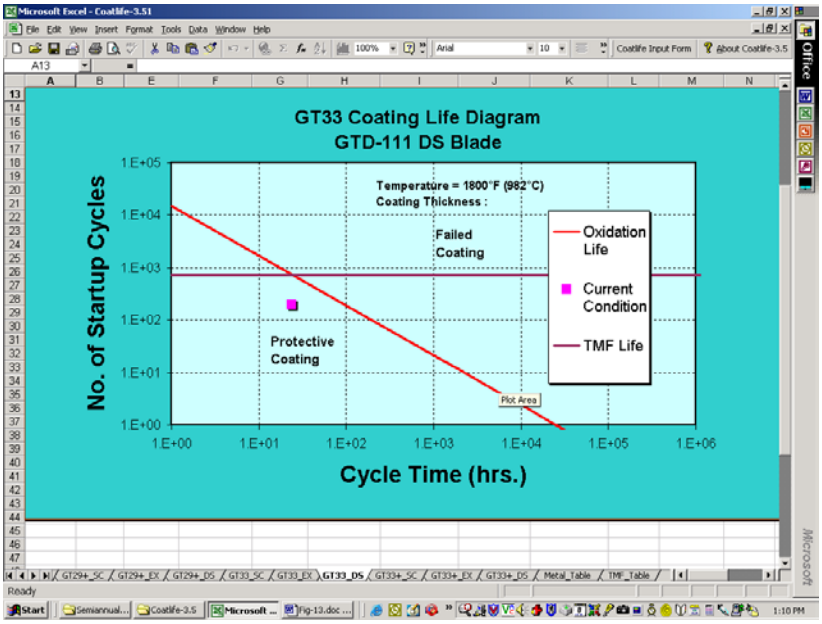

The application of COATLIFE 3.5 for lifing GT33/IN-738 was defined in the previous section. The data input for thermal cycling at a peak temperature of 1750°F (954°C) and a cycle time of 1000 hours for 40 cycles. The predicted oxidation life is 26.423 cycles at 1000 hr/cycle or 26,423 hours, as shown in Figure 5.8. The coating life diagram, shown in Figure 5.9, shows that the oxidation life (red line) has been exceeded, meaning the coating has failed by oxidation and Al depletion.

Figure 5.10 demonstrates the use of COATLIFE 3.5 for predicting coating life using NDE input data of volume percent of beta phase. For this example, the input data include the temperature (1800°F), cycle time (200 hours), and the volume percent of beta phase (20%) remained in the coating, the predicted coating life (failure cycles), percent life consumed, and the remaining life, which are shown at the right portion of the GUI, are 97.614 cycles, 50%, and 48.807 cycles, respectively. Thus, the remaining life of the coating is 9761.4 hours (48.087 cycles at 200 hours per cycle).

Figure 5.11 illustrates the use of COATLIFE 3.5 for predicting coating life using NDE input data of volume percent of Al content. For this example, the input data include the temperature (1800°F), cycle time (200 hours), and the atomic percent of Al content (11 at.%) in the coating, the predicted coating life (failure cycles), percent life consumed, and the remaining life, which are shown at the right portion of the GUI, are 97.614 cycles, 103.85%, and -3.7544 cycles, respectively. The negative remaining life means the coating has failed by oxidation and Al depletion. For this reason, the computed percent life consumed exceeded 100%.

Figure 5.8. Graphical-user Interface shows data input and predicted coating life for GT33/IN-738 subjected to thermal cycling at a peak temperature of 1750°F and a cycle time of 1000 hours for 40 start-up cycles. The TMF strain ranges are 30 cycles at 0.35%, 5 cycles at 0.45%, and 5 cycles at 0.55%. The predicted coating life, percent life consumed, and the remaining life are 26.423 cycles (or 26,423 hours), 151.38%, and -13.577 cycles, respectively.

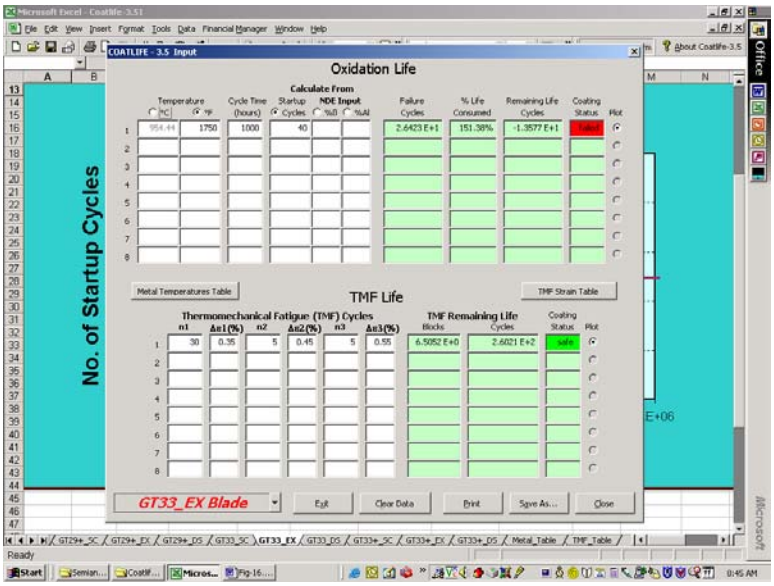

Figure 5.9. Predicted coating life diagram for GT33/IN-738 at 1750°F (954°C).

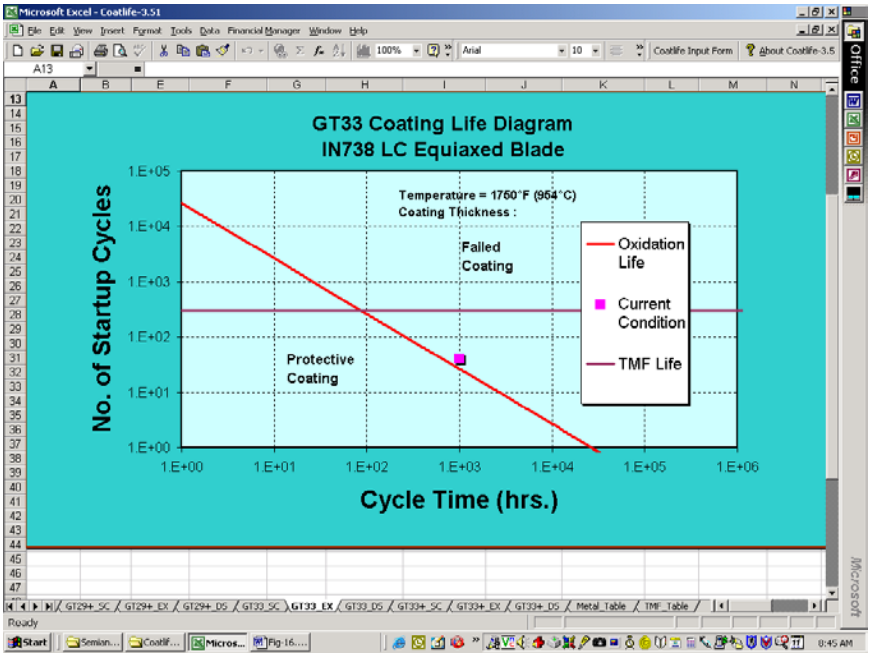

Figure 5.10. Graphical-user Interface shows data input of temperature (1800°F), cycle time (200 hours), and NDE input of 20% beta phase, together with the predicted coating life (97.614 cycles), percent life consumed (50%), and the remaining life (48.807 cycles) for GT33/GTD-111DS.

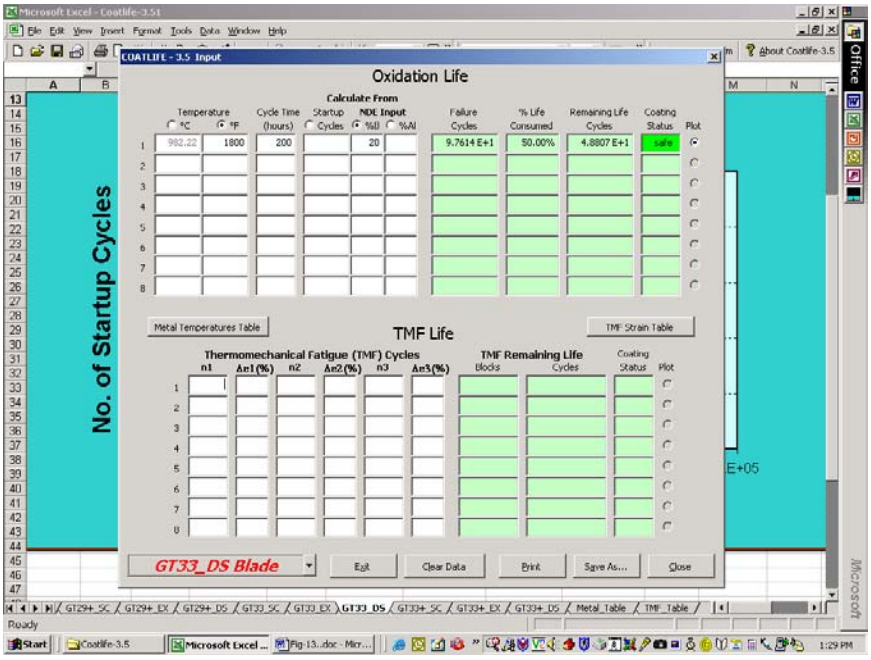

Figure 5.11. Graphical-user Interface shows data input of temperature (1800°F), cycle time (200 hours), and NDE input of Al content in atomic percent (11 at.%), together with the predicted coating life (97.614 cycles), percent life consumed (103.85%), and the remaining life (-3.7544 cycles) for GT33/GTD-111DS. A negative value for the remaining life means the coating has failed by oxidation and Al depletion.

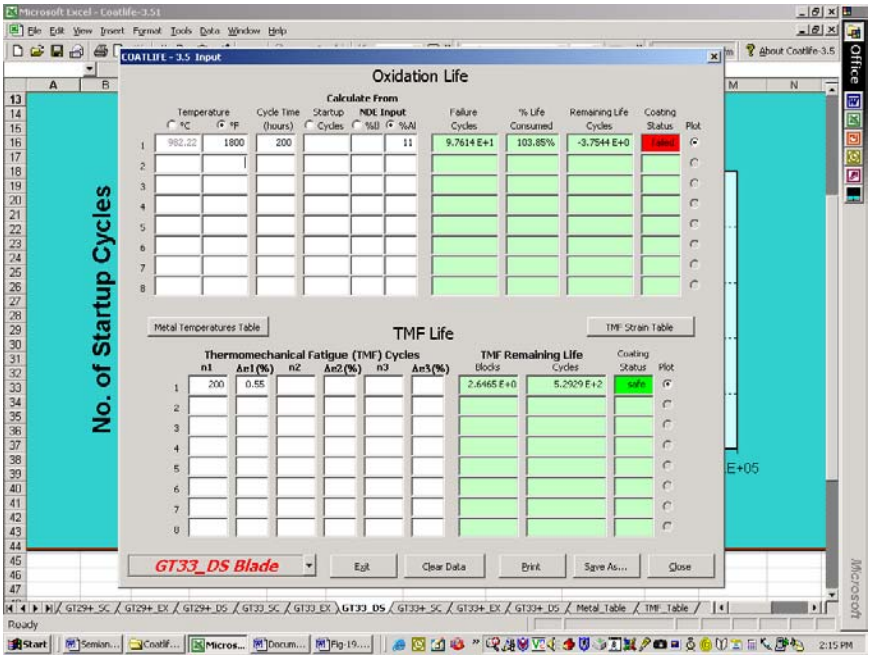

5.2D Task 3B Conclusions—MCrAlY Coating

- Considering the formation of chromium, aluminum, and yttrium rich oxides, the constants for COATLIFE were determined based on aluminum depletion in the coating.
- The calculated volume fraction of the remaining β-phase in the coating was in good agreement with the measured values of the specimens exposed at both peak temperatures.
- COATLIFE algorithm was validated for NiCoCrAlY (CT-102) coating. The graphical-user-interface (GUI) for COATLIFE Version 3.0 was revised to allow NDE input to calculate the coating life using the NDE measured data.
- Coating life diagrams for NiCoCrAlY (CT-102) coating were computed as a function of temperature. Both oxidation and TMF life equations were incorporated into COATLIFE Version 3.0.

6.0 Task 3 NDE of Coatings

6.1 Task 3.1 NDE System Assemblies and Testing

Eddy Current NDE for Coatings

During the reporting period, eddy current testing and characterization were conducted on one of two 2nd stage buckets that has undergone 24,000 hours of base-loaded operation with only 40 startups. This blade was taken out of service from 7FA+ turbine (7231FA) and is made of GTD 111 base material with GT 33+ duplex coatings. Unlike the other 1st stage buckets that have been cycled in peaking units, these came out of base-loaded units. Thus, no thermal mechanical fatigue cracking was observed from these second stage buckets.

Figure 6-1 shows an overall layout of the inspected 2nd stage bucket that has been gridded out for eddy current measurements.

Figure 6-1. Details of grid marks from pressure and suction sides of the 2nd stage bucket coated with GT 33+ coating

As shown in the figure, each grid box was approximately ½-inch square with alpha- numeric designation. The alphabets increased 1 through 20 (A-T) from the platform to blade tip, while the numbers increased (1-11 and 1-8) along the chord from the trailing edge to leading edge on the suction and pressure side of the blade, respectively, as shown. The number of maximum scans along the blade height was 20 scans from the chord positions #1 through 7, while the number dropped to 9 scans at chord position #8 on the pressure side. On the suction side, 20 scans were obtained from chord positions #1-8, 18 scans from chord position #9, 10 scans from chord position #10, and 3 scans from chord position #11.

As in the previous reporting, the normalized coil impedance versus frequency and normalized coil impedance versus chord position plots were used to assess, initially, the overall condition of the blade. Figure 6-2 shows two representative normalized coil impedance versus frequency plots from two different cross sections: Section E (close to 25% of the blade height) and Section O (close to 75% of the blade height).

On the surface, there were no obvious indications of major changes in the normalized coil impedance values. The slopes of the impedance curves were highest near the platform area, indicating the least amount of degradation to coating. At 75% of the blade height, there were reductions in the normalized coil impedance values accompanied by decrease in the slopes of normalized coil impedance curves. These changes are indicative of β-phase reduction in the topcoat.

Figure 6-3 shows normalized coil impedance values versus chord positions from Sections E and O. Higher normalized impedance values were observed at chord positions 3 through 7 where more normal coating conditions are found. Conversely, more reduced coil impedance values were noted at leading (chord positions 8 though 11) and trailing edges (chord positions 1 through 2). Between the two cross sections, more normal coating conditions were noted from the 25% location (Section E) than the 75% location (Section O).

Figure 6-2. Normalized coil impedance versus frequency at 25% and 75% of blade heights

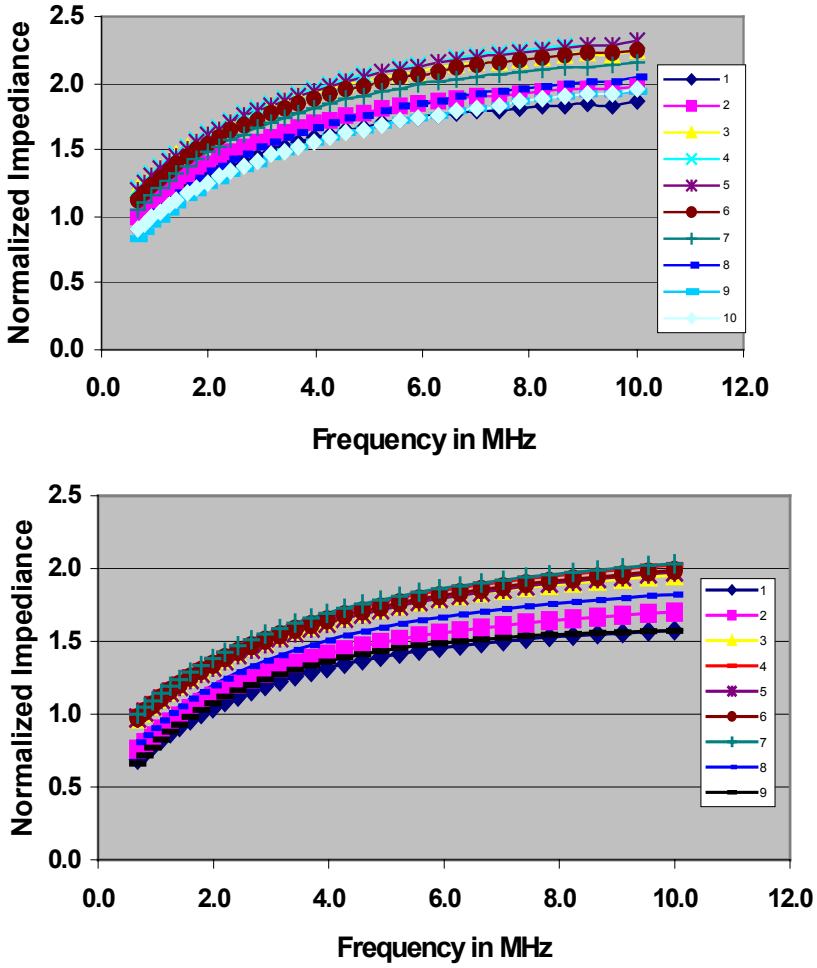

Figure 6-3. Normalized coil impedance versus chord positions at blade height E (25% height) and O (75% height) showing coating wear at both the leading and trailing edges

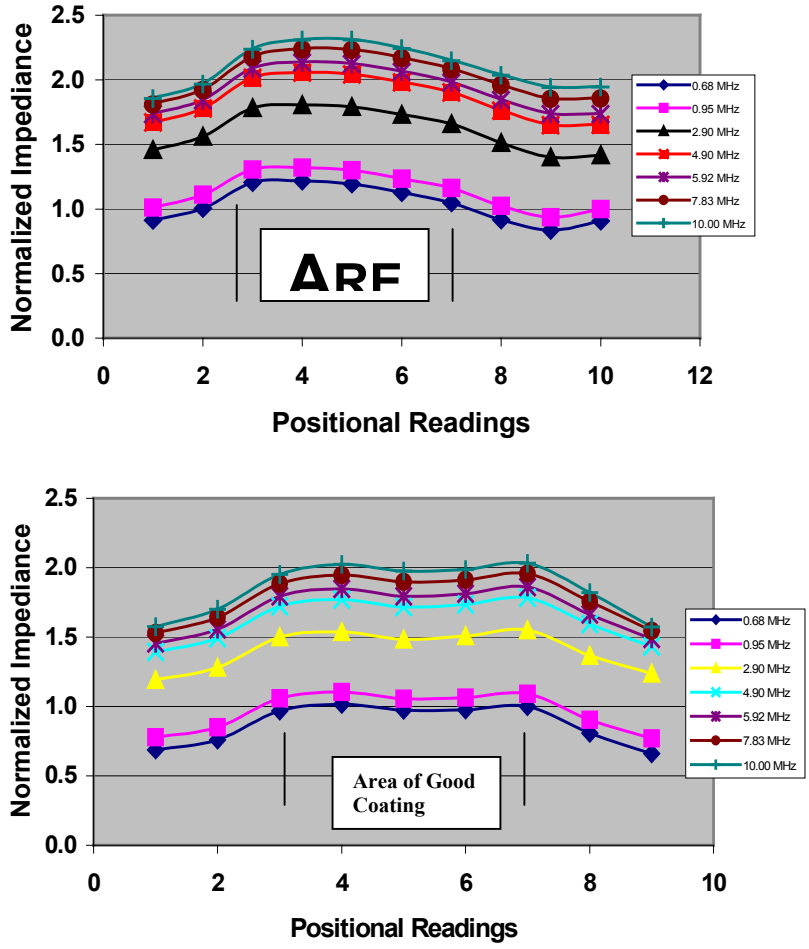

To quantify the remaining coat thickness, a three-layer inversion program was conducted on these two files containing normalized coil impedance values. Specifically, those values associated with topcoat thickness, combined topcoat and bond coat thickness, and conductivity of each layer was obtained. Table 6-1 shows those estimated values obtained from Section E representing more normal coating conditions.

Table 6-1. Calculated coating thickness and conductivity values from Section E

Chord Position	Topcoat L1 (um)	Topcoat + Bond Coat L2 (um)	Topcoat S1 (S/m*1e5)	Bond Coat S2 (S/m*1e5)	GTD 111 S1 (S/m*1e5)	Error (1e-3)
E1	41.5	202.4	8.71	9.34	7.86	2.329
E2	110.1	212.7	9.37	9.32	7.92	2.344
E3	201.5	256.9	9.7	8.02	8.12	2.407
E4	188.1	277	9.82	8.14	8.13	2.491
E5	181	333	9.84	8.17	8.1	2.006
E6	181.1	342.5	9.76	8.12	8.03	2.296
E7	182.5	296	9.63	8.16	7.93	2.183
E8	155.4	255	9.56	8.36	7.83	2.035
E9	168.2	397.5	9.45	7.89	7.77	1.839
E10	153	281	9.5	8.09	7.91	2.297

The estimated topcoat thickness values seem to be high – the nominal topcoat and the combined topcoat and bond coat thickness values were reported to be 50 and 300 microns, respectively. It is possible that current inversion algorithm is not able to reliably separate topcoat from bond coat thickness. Once actual coating values become available later this year, it will be possible to make additional refinements and corrections to the existing inversion program by using more robust inversion algorithm. Currently, these numbers can be used as references for comparative assessment of individual bucket Sections E and O.

Relying on the same initial conditions used to estimate thickness and conductivity values of Section E, the coating thickness and conductivity values were obtained from Section O. These calculated values are shown as Table 6-2.

Table 6-2. Calculated coating thickness and conductivity values from Section O

Chord Position	Topcoat L1 (um)	Topcoat + Bond Coat L2 (um)	Topcoat S1 (S/m*1e5)	Bond Coat S2 (S/m*1e5)	GTD 111 S1 (S/m*1e5)	Error (1e-3)
O1	16.8	215.1	0	8.89	7.67	1.021
O2	27.7	219.6	0	8.88	7.72	1.617
O3	118.1	216.7	9.46	8.99	7.92	1.534
O4	164.1	221.9	9.51	8.44	7.99	1.871
O5	160.6	217.4	9.46	8.43	7.96	1.629
O6	55.6	201.8	9.81	9.21	7.93	1.65
O7	52.6	204.8	9.94	9.25	7.94	1.98
O8	37	216.8	0	9	7.74	1.304
O9	2.5	238.9	0	8.87	7.56	1.15

What is interesting about this table is that zero topcoat conductivity values were obtained from chord positions 1 and 2, and 8 and 9. In general, this indicates absence of topcoat layers. The topcoat layer thickness column shows range of 2.5–37um of thickness remaining. These values may represent the low end of thickness values, which will result in no conductivity value estimates based on the current inversion algorithm. Once destructive validations are complete, additional refinements to inversion algorithm will be made.

Since no additional quantitative work can be done without additional destructive analysis results, the eddy current NDE focus shifted to better presentation of qualitative analysis results. This involved plotting of colored contour maps of the entire blade surface using calculated normalized impedance values, topcoat conductivity values, and topcoat thickness estimates. This means that it is no longer necessary to review just those cross sections, such as Section E and Section O. The entire blade surface can be viewed in its entirety.

Figure 6-4a shows a colored impedance map obtained at 10 MHz from the suction side of the entire blade surface. This figure shows normalized coil impedance plot with light yellow colors representing higher normalized coil impedance values representing areas of normal coatings. Conversely, darker blue colors represent lower coil impedance values representing possible areas of coating losses. At 10MHz, the coil impedance values are affected more by the outer topcoat conditions. Figure 6-4b shows calculated topcoat conductivity plot. Similarly, lighter yellow colors represent higher conductivity values while dark blue colors represent low to zero conductivity values.

Figure 6-4. Comparison of colored contour plots showing normalized impedance values at 10 MHz to calculated topcoat conductivity values from the suction side

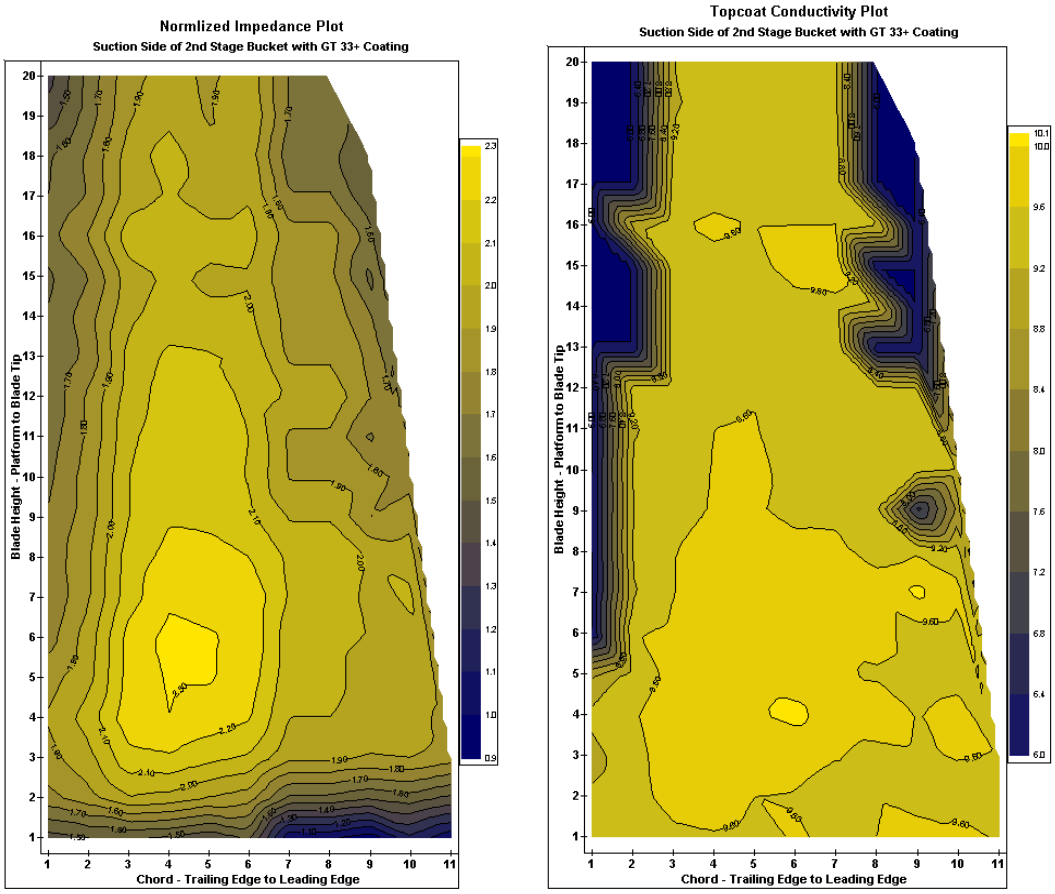

In general, higher normalized impedance values are correlated to higher conductivity values. In addition, the conductivity plot shows more definitively those locations of coating losses. On the trailing edge, the coating loss starts at elevation #5 (E) till the end of the bucket at elevation #20 (T), but more severe loss is evident at elevations #13 (M) through #20 (T). On the leading edge, a localized wall loss was noted at elevation # 9 (I). More severe coating loss was noted at elevations #13 (M) through #20 (T), very similar to conditions found at the trailing edge.

Figure 6-5 shows comparison of conductivity plot to topcoat thickness values. Unfortunately, there is no reliable correlation of locations of higher conductivity values to more normal coating thickness values. According to the conductivity plot, elevation #4 (D) shows higher conductivity values, while more normal topcoat thickness values are found at elevation #9 (I). As mentioned earlier, this maybe the limitation of the current inversion program to reliably separate thickness values of the topcoat layer from the bond coat layer. On the other hand, the locations of coating losses are well correlated. As mentioned before, both the trailing and leading edges are suffering from coating losses on the suction side.

Figure 6-5. Comparison of contour plots showing topcoat conductivity values to topcoat thickness values from the suction side

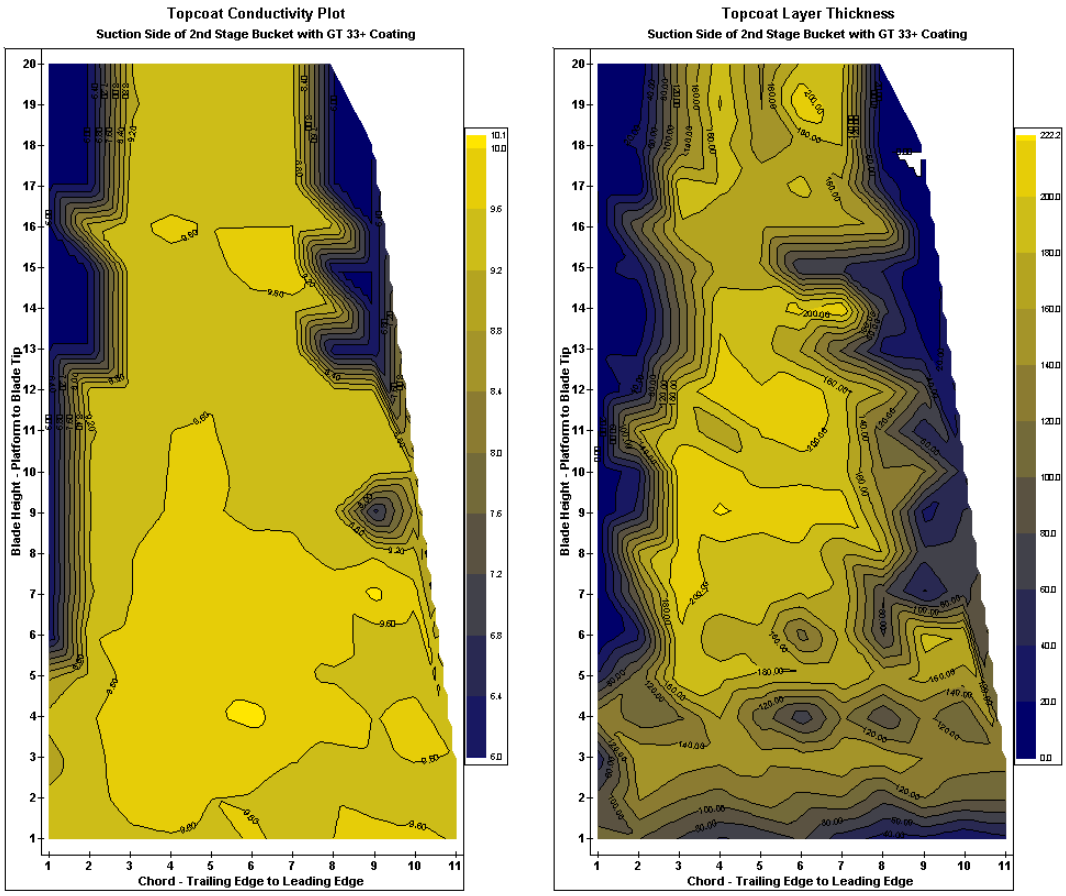

To complete the qualitative analyses, similar plots were prepared for the pressure side after calculating the thickness and conductivity values of each layer.

Figure 6-6 shows comparison of normalized impedance plot at 10 MHz to topcoat conductivity plot from the pressure side. As in the suction side, there is a general agreement of locations where higher normalized impedance values are correlated to higher topcoat conductivity values. More normal coating conditions were found along the leading edge, while localized wall losses were noted at the trailing edges at elevations #17 (Q) through #20 (T).

Figure 6-6. Comparison of colored contour plots showing normalized impedance values at 10 MHz to calculated topcoat conductivity values from the pressure side

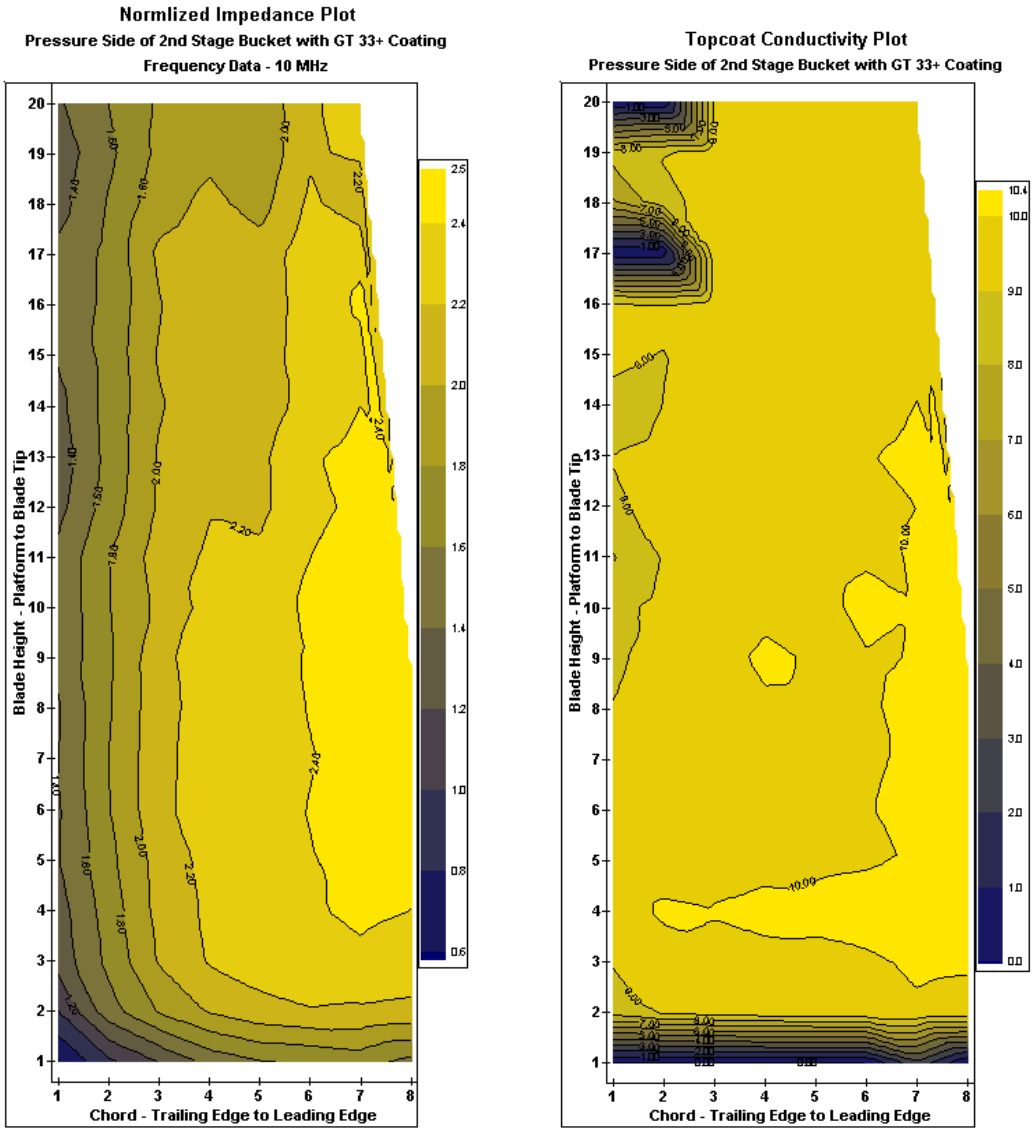

Figure 6-7 shows comparison of plots showing topcoat conductivity values to topcoat thickness values on the pressure side. Even though there is some correlation of normal coating to higher conductivity at elevation #11(K) but it is not the same at elevation #4 (D). At this elevation, the same high conductivity value is correlated to one-half of the thickness value obtained from the #11 elevation. So, once again, the topcoat thickness estimates need to be improved.

As for coating losses, both plots agree on the locations as shown by the similar presence dark blue colors.

Figure 6-7. Comparison of contour plots showing topcoat conductivity values to topcoat thickness values from the pressure side

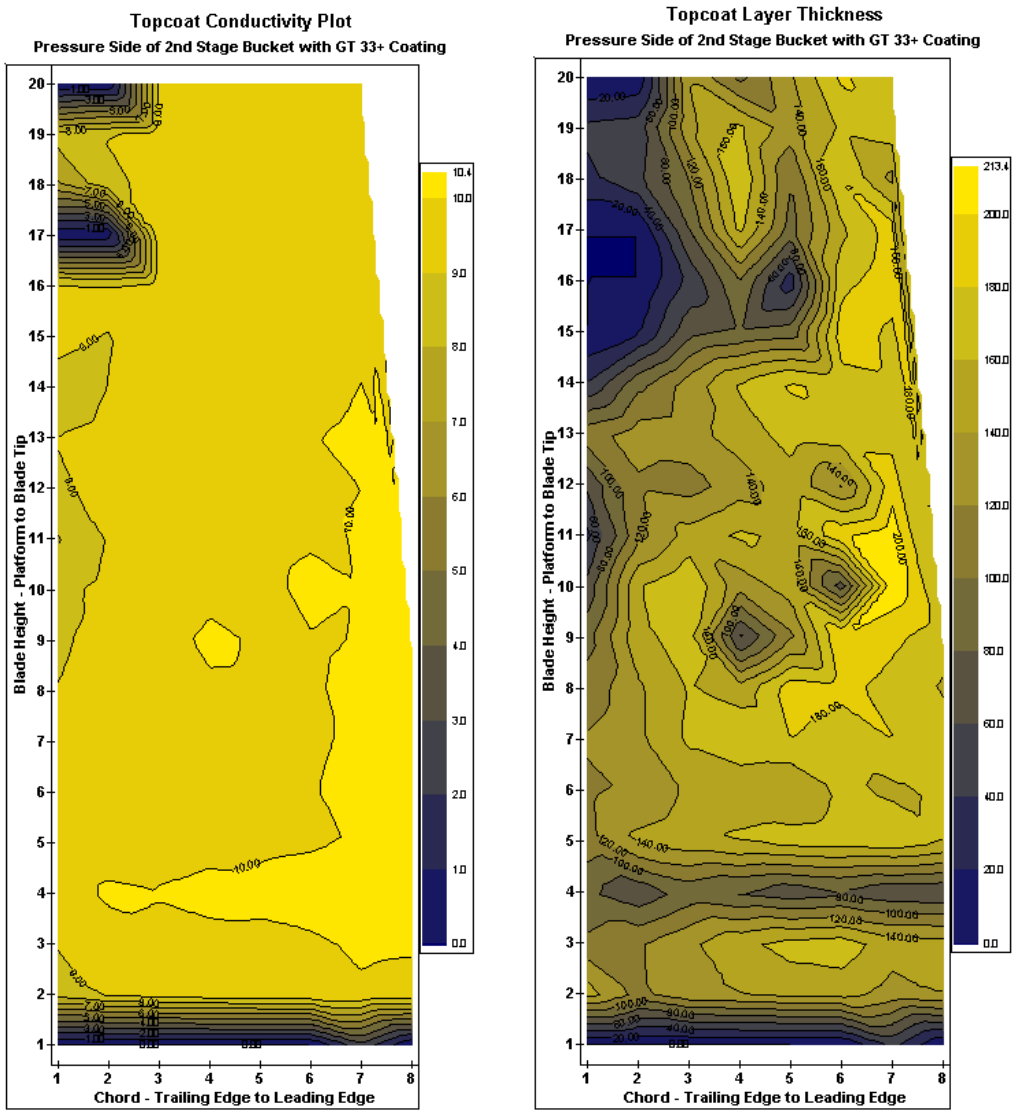

X-ray Florescence NDE for Coatings

While waiting for destructive analysis results from the 2nd stage bucket, an attempt was made to determine nondestructively the remaining aluminum content of the duplex metallic coatings, GT 33+, by x-ray florescence technique. X-ray florescence (XRF) is a nondestructive testing method for the elemental analysis of solids and liquids. XRF measurements are performed by illuminating a portion of the sample with x-rays and measure the energy and count rate of the fluoresced x-rays. Incident x-ray photons cause electrons to be ejected from atoms in the test sample. As the remaining electrons fill the newly created vacancies, excess energy from vacating electrons is emitted as x-rays. The energy of these fluoresced x-rays corresponds to the energy change of the electron transition, and each element fluoresces at a characteristic set of energies. X-rays resulting from the most probable

transitions terminating in the K shell are known as "aK" x-rays, and x-rays resulting from the most probable transitions terminating in the L shell are known as "aL" x-rays. Fluorescence occurring due to direct excitation by x-rays from the x-ray source is known as "primary fluorescence". Fluorescence from an atom excited by x-rays fluoresced from the other elements in the sample is known as "secondary fluorescence". For this testing, fluoresced x-ray energies and rates are measured with a solid-state energy-dispersive detector. The energies of these emitted x-rays are used to identify the elements present in the sample while the concentrations of the elements are determined by the intensity of the x-rays. With proper calibration, the various elements present and their concentrations can be determined. What was attempted involved testing and comparison of results obtained from an as-coated test specimen to those thermally aged test samples using a portable XRF system shown as Figure 6-8.

Figure 6-8. EDAX Eagle II X-Ray Florescence System

Preliminary results showed that some of key coating elements were observed at the following energy levels: CoK @ 1 keV, AlK @ 1.4865 keV, RhL @ 2.6944 keV, CrK @ 5.4101 keV and Nik @ 7.4695 keV.

Figures 6-9 and 6-10 show examples of elemental images of the as coated and the aged sample at 1850°F with 4000 cycles.

Figure 6-9. Elemental Images at Different Intensity Levels for As-coated Test Sample

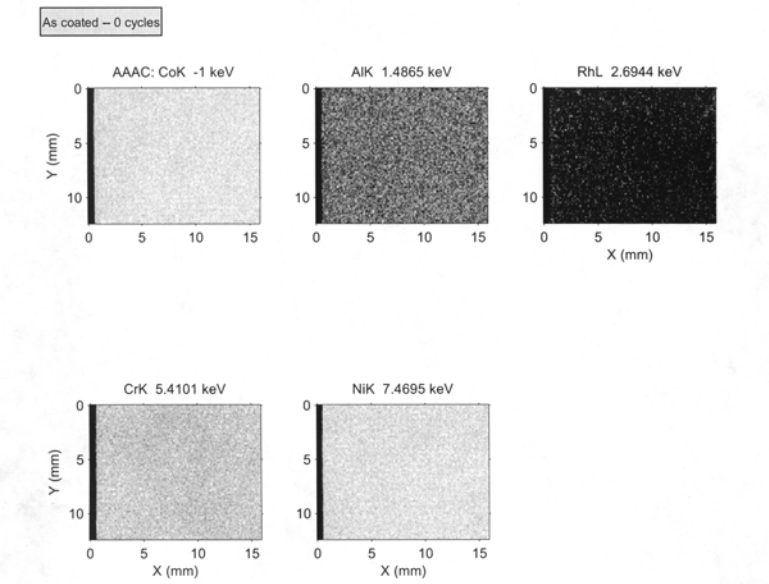

Figure 6-10. Elemental Images at Different Intensity Levels for Aged Test Sample - 1850°F with 4000 Cycles

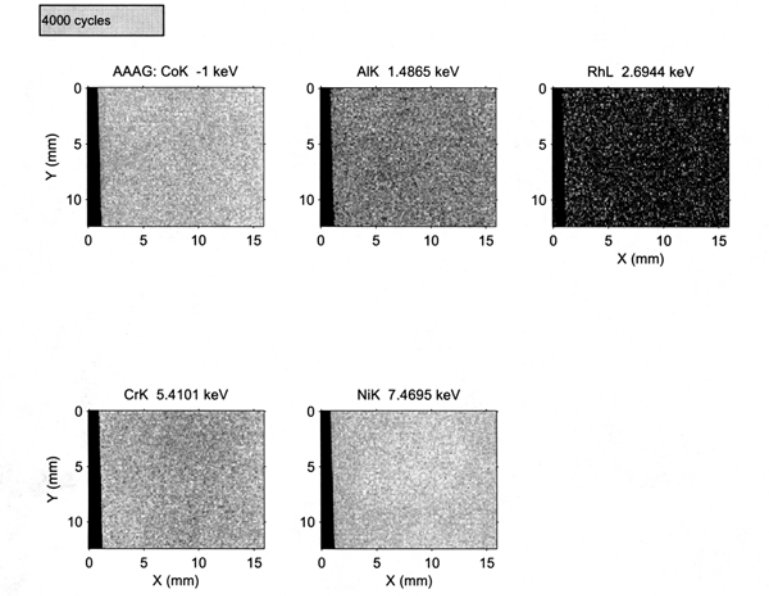

Other aged GT 33+ coated test samples consisted of the following conditions: 1850°F with 600 cycles, 1850°F with 1500 cycles, 1850°F with 2400 cycles, and 1850°F with 4000 cycles. When spectrum analyses were conducted aluminum was found to be higher on the aged samples in comparison to the as-coated sample. This was just the opposite of what was expected. Also, there

were no significant changes in the aluminum intensity levels from the 600-cycle coupon to 4000-cycle coupon.

Figure 6-11 shows the mean intensity levels of aluminum versus thermal aging cycles.

One explanation for the lower intensity aluminum level for the as coated is that tested side may have been stripped of the coating. This would cause the aluminum reading to be lower due to low aluminum Wt.% of around 3% for GTD 111 versus 24% for topcoat.

As for no apparent change in the aluminum intensity levels for the aged samples, this may be caused possibly by changes in the other elements, such as Cr, Co, Ni, and Ti, which may affect the aluminum intensities due to absorption. Additional investigation will be conducted to determine this apparent lack of changes in the aluminum intensity levels.

Figure 6-11. Mean Aluminum Intensity Levels versus Thermal Aging Cycles.

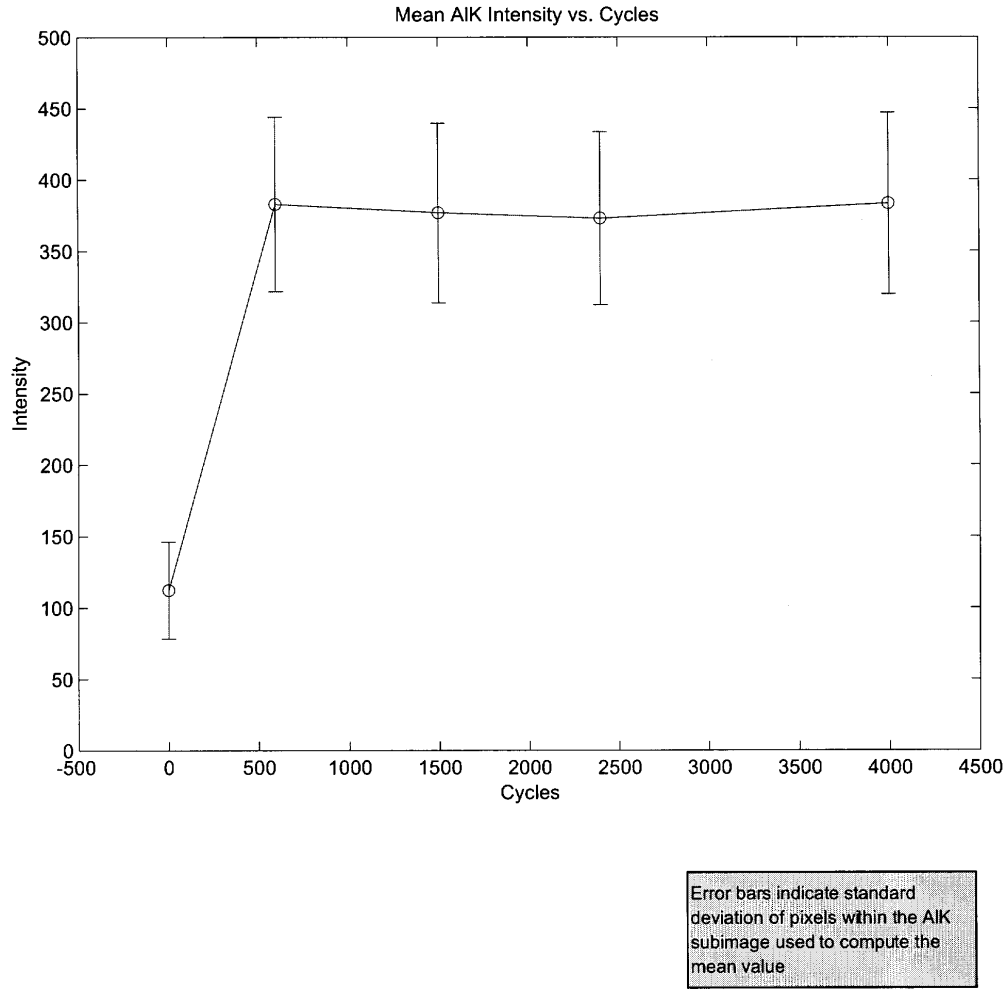

6.2 Conclusions—Task 3

For aged duplex coating, the application of eddy current NDE has already demonstrated its capability to provide qualitative assessment of coating conditions by separating normal coating, β-phase depleted coating, and defective coating with thermal mechanical fatigue cracking. In addition, using a three-layer inversion program, quantitative assessment was made by calculating conductivity values associated with topcoat, bond coat, and GTD 111 substrate.

During the reporting, much progress has been made in the data display presentation by plotting colored contour maps of those calculated parameters, such as normalized impedance values, conductivity values, and coating thickness values. By reviewing the colored contour map of the entire bucket, it's easier to see where the problem is taking place. These colored contour maps showed general agreement of locations where high normalized impedance values were correlated to high conductivity values.

To extend the quantitative assessment to coating thickness estimates, the current three-layer inversion program encountered some difficulty separating the topcoat thickness layer reliably from the bond coat thickness layer.

To improve on the current quantitative assessment of coating thickness and conductivity values, enhancement to the current software will be made later this year. This software upgrade will increase the number of layers available for modeling from three layers to four layers. In addition, the upgrade will allow us to evaluate TBC coatings. The current software intentionally minimize lift-off variable but in the new upgrade, this lift-off value can be used to assess thickness of the non-conductive ceramic coatings, including the TGO layer. Also, the new software will be conducive to the use of a flexible probe for next year's field demonstration.

7.0 TASK 4. FIELD VALIDATION OF COATLIFE AND NDE

Objective

The objective of this task is to validate the predictive capabilities of COATLIFE and the eddy current NDE methodology on field-operated coated turbine buckets. This task is scheduled to begin in Nov 2003.

Results

Blade procurement under this task started in January 2002. A TBC coated and service run blade was procured. The operating history of the blade is as follows:

- ISO Turbine Inlet Temp (TIT) - 1110°C
- Operating Hours - 15,000 hrs
- No. of Starts - 52
- No of Trips from 1050C or higher TIT - 3
- No of Trips from below 1050C TIT - 1

- No of Protective Load Shedding from 1050C or higher TIT - 15
- No of Protective Load Shedding from below 1050C TIT - 11
- No of Low Load Cycles (i.e. when TIT drops below 1050C) - 137 cycles
- Power Augmentation History - 206 cycles, 339 hrs
- Equivalent Operating hours - 18,900 EOH

The blade had operated on a Alstom 13E2 turbine. The blade was shipped to EPRI Center at Charlotte for NDE evaluations. It is necessary to procure a TBC coated blade that operated in an advanced engine (G or H class) with a higher TIT than 1110°C.

8.0 TASK 5. ECONOMIC RISK-BASED DECISION ANALYSIS

Task 5 work is on hiatus pending the completion of the blade coating metallurgy work (Task 2), NDE work (Task 3), and the final modifications to the COATLIFE software. During this reporting period, a software specification was defined for the economic analysis of the hot section buckets.

9.0 REFERENCES

1. R. A. Miller, "Life Modeling of Thermal Barrier Coatings for Aircraft Gas Turbine Engines", J. of Engineering for Gas Turbines and Power, Vol. 111, April, 1989.
2. R. Viswanathan, "Blade Life Management: Coating Systems", EPRI Report 1006608, 2002.
3. *ANSYS User's Manual,* ANSYS Inc., Revision 5.6, 2000.